COMBINED TENSION AND TORSION TESTING OF ALUMINUM AND POLYETHYLENE

by

Sami Korkmaz

B.S. in M.E., Boğaziçi Üniversitesi, 1983

Submitted to the Institute for Graduate Studies in Science and Engineering in partial fulfillment of the requirements for the degree of

Master of Science

in

Mechanical Engineering

Boğaziçi Üniversitesi

1985

COMBINED TENSION AND TORSION TESTING

OF ALUMINUM AND POLYETHYLENE

APPROVED BY:

Doç.Dr. Sabri Altıntaş: S.Altıntaş.....
(Thesis Supervisor)

Doç.Dr. Burak Erman : Burak Erman.....

Prof.Dr. Kâşif Onaran : K. Onaran.....

DATE OF APPROVAL: 18.11.1985

ACKNOWLEDGEMENTS

I would like to express my sincere thanks to my thesis supervisor Doç. Dr. Sabri Altıntaş for his precious guideance and invaluable contributions throughout the preparation of this study.

I express my appreciation to Prof. Dr. Kâşif Onaran and Doç. Dr. Burak Erman for their precious guideance in my works.

I also want to thank to İstinye Tersanesi for their helps in preparing the samples.

October, 1985 Sami Korkmaz

COMBINED TENSION AND TORSION TESTING OF ALUMINUM AND POLYETHYLENE

In this study, the plastic deformation behaviour of five different types of materials have been investigated by performing combined tension and torsion experiments on thin-walled tubular specimens. The effects of annealing, cold working and age hardening on the yield curves of aluminum have been determined. Casted aluminum and polyethylene specimens were also tested under the same stress conditions. The validity of theoretical yield criteria and the normality condition of the plastic strain vector to the yield curves have also been investigated. It was observed that Mises criterion yielded better representation for the yield curves of the isotropic materials.

ÖZET

Bu çalışmada, ince cidarlı boru numuneye birleşik çekme ve burma gerilmeleri uygulayarak beş değişik malzemenin plastik şekil değiştirme davranışları araştırıldı. Tavlama, soğuk şekil değiştirme ve yaşlandırma sertleştirmesinin aliminyumun akma eğrileri üzerindeki etkileri tespit edildi. Aynı gerilme koşulları altında dökme aliminyum ve polietilen malzemeler de incelendi. Ayrıca, teorik akma koşullarının ve plastik şekil değiştirme vektörünün akma eğrisine olan normallik koşulunun geçerliliği araştırıldı. Mises koşulunun isotrop malzemelerin akma eğrilerine daha iyi uyduğu gözlendi

TABLE OF CONTENTS

LIST OF FIGURES

LIST OF TABLES

LIST OF SYMBOLS

Symbol	Definition
σ	normal stress
σ_1 , σ_2 , σ_3	principle stresses
σ_1' , σ_2' , σ_3'	deviator stress tensor
σ_m	hydrostatic stress $\sigma_m=(\sigma_1+\sigma_2+\sigma_3)/3$
τ	shear stress
J_1 , J_2 , J_3	first three invariants of σ_{ij}
J_1' , J_2' , J_3'	cuadratic invariants of the deviator stress tensor
k	characteristik value of material
Y	yield stress in pure tension
ε	axial strain
γ	shear strain
N , F	axial force
p	hydrostatic pressure
$\bar{\varepsilon}$	equivalent strain
$\bar{\sigma}$	equivalent stress
σ_a	axial stress
σ_c	circumferencial stress
t_w	wall thickness
T	torsion
$\bar{t}$	average thickness

I. INTRODUCTION

The plastic response of metals to multiaxial stresses has been of interest for many years. The concept of effective stress and strain (1)* is used to reduce multiaxial response to a universal stress-strain curve, typically that measured in uniaxial tension. The von Meses isotropic yield and flow criterion is the most commonly used criterion for stress analysis. He suggested, in 1913, that quadratic invariant of the deviator stress tensor, J_2', should be considered as a yield criterion. If

$$J_2' = [(\sigma_1' - \sigma_2')^2 + (\sigma_2' - \sigma_3')^2 + (\sigma_3' - \sigma_1')^2]/6 < k^2$$

yielding will not occur. Here k^2 is a characteristic value of material. This relation was also proposed by Huber (2) in 1904 and apperantly by Maxwell in a letter to Kelvin as early as 1856. Tresca suggested, in 1864, that yielding occurs when the maximum value of the extremum shear stresses in the material attains a critical value. His relation is easy to use.

The classical experimental work of this kind was performed in 1931 by Taylor and Quinney which was intended to solve this problem. They used cupper, mild steel and aluminum thin-walled tubes, which were said to be very nearly isotropic and tested them in combined tension and torsion. They observed deviations from the theoretical curves and concluded that these discrepancies were real and could not be attributed to

* Numbers in paranthesis indicates references at the end of the paper.

experimental error or anisotropy of the specimen material. Similar results were obtained earlier, for example by Lode (who used the thin-walled tube as the first time) in 1926 by Ros and Eichinger in 1929 and in 1953, by Siebel who employed combined bending and torsion. An extensive survey of literature with this topic up to about 1976 was presented by Hecker in the table 1 (3).

A standard simple tension test at room temperature gives the well-known stress-strain curve of figure 1. The initial elastic region appears as straight line extending to quite high values of stress for structural metals. Above the yield point, the response of the metal is both elastic and plastic. Unloading at any stage reduces the strain along an elastic unloading line. Reloading retraces the unloading line with relatively minor deviation, and then produces plastic deformation.

The definition of yield employed is very important since different yield surfaces result from different definitio Figure 1 shows some of the possible definitions which have been used and are currently in use. These are

A. The proportionality limit

B. 10-15 $\mu\varepsilon$ Plastic strain offset

C. The conventional engineering offset of 0.2 percent strain

D. Point of tangency stress-strain curve with a multiple of elastic slope

E-F. Extrapolation methods (Taylor-Quinney) definitio

In this study 10-15 micro inch per inch plastic strai offset type yielding definition was used.

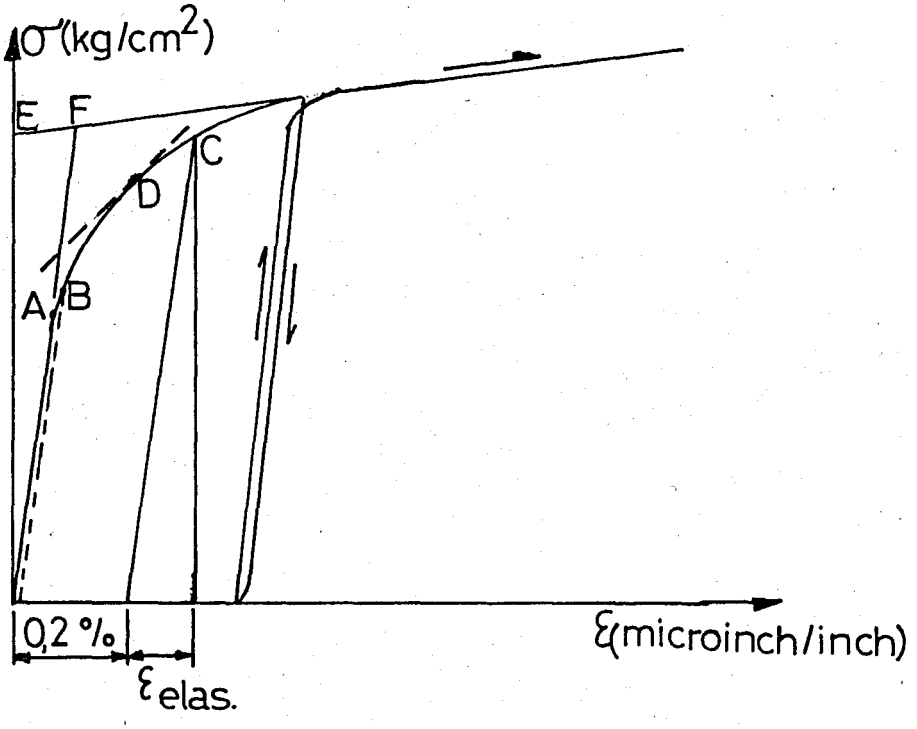

A - Deviation from linearity

B - Small measurable offset

C - 0,2 % offset

D - Slope equal to a constant elastic slope

E - Extrapolation of post yield slope to ordinate

F - Intersection of elastic slpe & definition E.

Figure 1. Various definitions of yield.(3)

Table 1. Review of subsequent yield loci work (3)

Investigators	Year	Specimen type and loading	Materials
1. Naghdi, Essenburg and Koff	1958	tubes, tension-torsion	2024-T4 Al
2. Hu and Bratt	1958	Tubes, Tension-I.P.	1100-0 Al
3. Lagn and Shismarov	1958	Tubes, Tension-Torsion	Nickel
4. Mc Comb	1960	Tubes, Axial-Torsion	2014-T4 Al
5. Talypov	1961	Tubes, Axial-I.P.	Low-C Steel
6. Ivey	1961	Tubes, Axial-Torsion	2024-T4 Al
7. Shismarev	1962	Tubes, Axial-Torsion	Alloy steel
8. Bertsch and Findley	1962	Tubes, Tension-Torsion	6061-T6 Al
9. Wells	1963	Tubes, Tension-Torsion	35-Al
10. Szczepinski	1963	Prestrained sheet, tension	Al-4.5Mg Alloy
11. Parker and Basset	1963	Tubes, I.P.-Torsion	70-30 Brass
12. Bui	1964	Tubes, Axial-Torsion	Pure Al Armco F
13. Mair and Pugh	1964	Tubes, Tension-Torsion	Pure Cu, Anneal
14. Jenkins	1965	Tubes, Axial-Torsion Axial-I.P.	Zinc-Alloy (Zamak-3)
15. Miastkowski and Seczepinski	1965	Tubes, Tension-I.P.	63-37 Brass Annealed
16. Haythorthwaite et al	1966	Tubes, Axial-I.P.	1045 Steel
17. Panov	1966	Tubes, Axial-Torsion	Low-C Steel, Annealed
18. Dudderar and Duffy	1967	Tubes, Tension-Torsion	Neutron irrad. Cu

Table 1. (Continued)

Investigators	Year	Specimen type and loading	Materials
19. Miastkowski	1968	Tubes, Tension-I.P.	63-37 Brass
20. Shiratori, Ikegami and Okano	1968	Cross-Shaped sheet	Half-hard BsP3 Brass
21. Szczepinski and Miastkowski	1968	Prestrained sheet, Tension	PA-3 Al, Annealed
22. Shiratori and Ikegami	1968	Cross-Shaped sheet	BsP3 Brass Half -hard
23. Phillips	1968	Tubes, Tension-Torsion RT to 150°C	6061-T6 Al
25. Igaki, Sugimoto and Saito	1970	Tubes, Axial-I.P.	65-35 Brass
26. Bui	1970	Tubes, Axial-Torsion	Pure Al, Pure Cu
27. Williams, Svenson	1970	Tubes, Tension-Torsion	1100-0 Al
28. Babcock et al	1970	Tubes, Axial-I.P.-E.P.	2024-T3 Al
29. Lindholm	1970	Tubes, Tension-Torsion-Internal Pressure	S-200E Be Ti-6Al-4V
30. Hecker	1971	Tubes, Tension-I.P.	1100-0 Al OFHC Cu
31. Lebednev, Novikov	1971	Tubes, Axial-I.P. -180° C to R.T.	0.37 pencent C -steel, Cast iron, Al
32. Tozawa, Nakamura and Shinkai	1971	Tubes, Tension-I.P.	BsBM-2 Brass, Annealed
33. Hecker	1972	Tubes, Axial-I.P.	1100-0Al OFHC Cu

Table 1. (Continued)

Investigators	Year	Specimen type and loading	Materials
34. Shirators, Ikegami and Kaneko	1972	Tubes, Axial-Torsion I.P.-E.P.	BsBM-2 Brass, Annealed
35. Phillips, Lui and Justusson	1972	Tubes, Axial-Torsion R.T. to 150°C	1100-O Al
36. Phillips and Tang	1972	Tubes, Axial-Torsion R.T. to 150°C	1100-O Al
37. Berio et al	1972	Prestrained sheets, Tension	Low-C steel
38. Bui	1972	Tubes, Axial-Torsion	Pure Al, Pure Cu, Armco Fe
39. Hecker	1973	Tubes, Axial-I.P.	1100-O Al OFHC Cu
40. Pillips	1973	Tubes, Axial-Torsion	1100-O Al
41. Phillips and Kasper	1973	Tubes, Axial-Torsion R.T. to 150°C	1100-O Al
42. Michno and Findley	1973	Tubes, Axial-Torsion	304-L Stainl. Steel
43. Shiratorl, Ikegami and Okano	1973	Tubes, Axial-Torsion, Internal Pressure	BsBM-2 Brass
44. Liu	1974	Tubes, Axial-Torsion R.T. to 1250°F	203 stainl. steel
45. Hecker	1974	Tubes, Axial-I.P.	1100-O Al 1100-H19 Al OFHC Cu
46. Marjanovic, Szczepinski	1974	Tubes, Axial-I.P.	63-37 Brass, Annealed

Table 1. (Continued)

Investigators	Year	Specimen type and loading	materials
47. Phillips, Tang and Ricciuti	1974	Tubes, Axial-Torsion R.T. to 150°C	1100-O Al
48. Döner, Chang and Conrad	1974	Tubes, Tension-Torsion	OFHC Cu
49. Marjanovic and Szczepinski	1975	Tubes, Axial-I.P.	63-37 Brass, Annealed
50. Michno and Findley	1975	Tubes, Axial-Torsion	1017 Steel
51. Phillips and Ricciuti	1976	Tubes, Axial-Torsion R.T. to 150°C	

The curves which join the experimental yield points, called as "yield curve". Initial yield curve joins the initial yield points. The points determined by probing beyond the initial yield points give the subsequent yield curves. Fig.2 shows the initial and subsequent yield curves for isotropic and anisotropic strain hardening materials.

Any specimen which is deformed appreciably in the plastic range will be "strain hardened", and its properties at a later stage will be quite different from the original properties of the material. This is due to the strain hardening character of the material.

By considering the full combination of twisting moment, axial force, and internal pressure, the initial

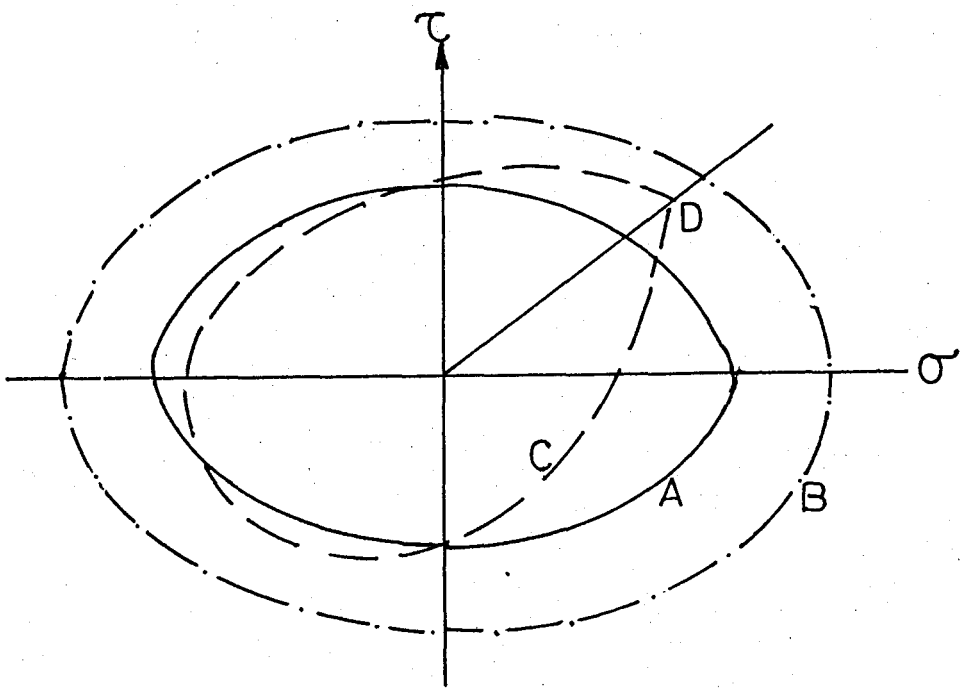

A-Initial yield curve

B-Isotropic strain hardening material

C-Anisotropic strain hardening material
(Real material)

D-Yield corner

Figure 2. Initial and subsequent yield curves.(4)

yield points determined from the tests on thin-walled tubes form a surface (Yield Surface) in the tree dimensional space. Figure 3 A shows the yield surface for combined tension, torsion and internal pressure.

All yield curves are found to be convex. As a consequence, rather few points can determine the position of the curve with reasonable accuracy. If neighboring points

are known, as shown in Figure 3 B the location of a new point must lie on or in the shaded triangle.

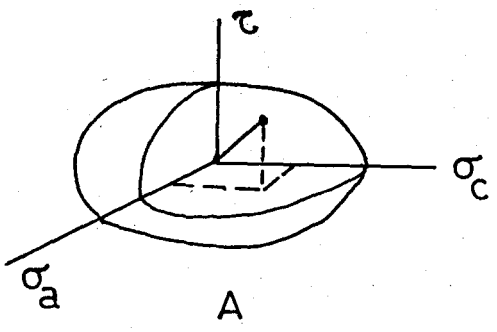

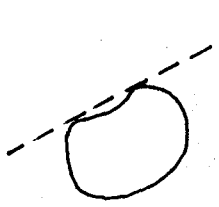

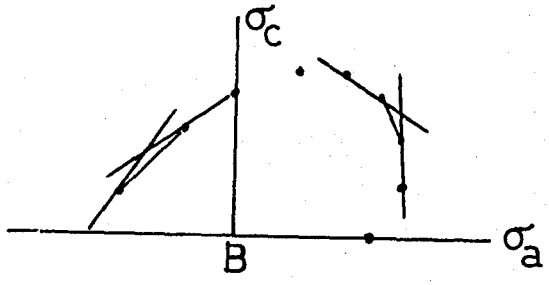

Figure 3. A-Yield surface

B-Yield curves are convex.(4)

Incremental strain vectors are perpendicular to yield curve. This is named "Normality". Normality of the strain vector and convexity have been established experimentally in several studies (3)

In this study, four different kinds of Aluminum materials and a polyethylene sample was tested under combined tension and torsion loadings. Initial and subsequent yield curves were plotted experimentally and they have been

compared with theoretical curves. Also the effects of heat treatments and anisotropy on the yielding behaviour of the materials under combined tension and torsion was investigated.

II. YIELD CRITERIA FOR DUCTILE METALS

When a body is subjected to a system of external forces the body is stressed and it deforms. If the forces are relieved then the stresses are relieved and the body may regain its original shape. In this case, the deformation is recoverable or reversible and is referred to as elastic deformation. The associated stresses and strains are elastic stresses and strains.

However, the external forces may be of such magnitudes that, when relieved, the deformation is not entirely recoverable and the body does not regain its original shape. In this case, plastic, non-recoverable or irreversible deformation has occured. The stresses thus attain a value which exceeds that required for elastic deformation and the material is said to have yielded.

A material is homogeneous if its properties do not vary from element to element and the material is isotropic if its properties are independent of the orientation of the system of coordinate reference axes chosen and therefore independent of direction. The original workpiece material subsequently used in a metal forming process may be regarded as being essentially homogeneous and isotropic and it remains so during elastic deformation up to the onset of yield.

Nevertheless, during plastic deformation, the workpiece material will tend to become increasingly anisotropic and inhomogeneity may be introduced.

2.1. General Considerations (5)

A yield criterion may be defined as a hypothesis concerning the limit of elastic deformation due to any possible stress state. By means of a yield criterion it is then possible to decide whether plastic deformation takes place or, indeed, is possible. Any proposed yield criterion should be verified experimentally.

If the material is isotropic, plastic yielding can then only depend on the magnitudes of the three principle stresses and not on their directions. Any yield criterion can thus be expressed in the form,

$$\phi(J_1, J_2, J_3) = 0 \qquad [1]$$

where J_1, J_2, J_3, are the first three invariants of the stress tensor σ_{ij}.

$$J_1 = \sigma_x + \sigma_y + \sigma_z$$
$$J_2 = (\sigma_x\sigma_y + \sigma_y\sigma_z + \sigma_z\sigma_x) + (\tau_{xy}^2 + \tau_{yz}^2 + \tau_{zx}^2)$$
$$J_3 = \sigma_x\sigma_y\sigma_z + 2\tau_{xy}\tau_{yz}\tau_{zx} - (\tau_{yz}^2\sigma_x + \tau_{zx}^2\sigma_y + \tau_{xy}^2\sigma_z)$$

In terms of the principle stresses which are the roots of the cubic equation,

$$\sigma^3 - J_1\sigma^2 - J_2\sigma - J_3 = 0$$

The stress invariants are

$$J_1 = \sigma_1 + \sigma_2 + \sigma_3$$

$$J_2 = -(\sigma_1 \sigma_2 + \sigma_2 \sigma_3 + \sigma_3 \sigma_1)$$

$$J_3 = \sigma_1 \sigma_2 \sigma_3$$

It has been shown experimentally by Bridgman (6), who performed tensile tests on both metallic and nonmetallic materials subjected to very high hydrostatic pressures of the order of 25000 atm, that some materials are compressible to a significant extent. For the range of pressures usually encountered during metal forming processes the degree of compressibility was found to be very small.

It may therefore be assumed that for a moderate hydrostatic stress, either compressive or tensile, and whether applied alone or superimposed on a combined stress state, the yielding of a metal is unaffected. Equation [1] may therefore be simplified by stating the yield criterion in terms of the invariants of the deviator stress tensor, σ_{ij}', so that

$$\phi(J_2', J_3') = 0 \qquad [2]$$

since $J_1' = 0$ (5)

$$J_2' = -(\sigma_1'\sigma_2' + \sigma_2'\sigma_3' + \sigma_3'\sigma_1') = [(\sigma_1')^2 + (\sigma_2')^2 + (\sigma_3')^2] / 2$$

$$J_3' = \sigma_1'\sigma_2'\sigma_3' = [(\sigma_1')^3 + (\sigma_2')^3 + (\sigma_3')^3] / 3$$

where

$$\sigma_1' = \sigma_1 - \sigma_m$$

$$\sigma_m = (\sigma_1 + \sigma_2 + \sigma_3) / 3$$

$$\sigma_1' = \sigma_1 - (\sigma_1 + \sigma_2 + \sigma_3) / 3$$

or $$\sigma_1' = (2\sigma_1 - \sigma_2 - \sigma_3) / 3$$

similarly $$\sigma_2' = (2\sigma_2 - \sigma_3 - \sigma_1) / 3$$

$$\sigma_3' = (2\sigma_3 - \sigma_1 - \sigma_2) / 3$$

An idealised plastically deforming body does not exhibit a Bauschinger effect which implies that the magnitude of the yield stress is the same in tension and compression. Consider an element to be relieved from a plastic stress state, σ_{ij} , and then restressed to the state, $-\sigma_{ij}$, keeping the ratio of the stress components constant throughout. The condition assumed is that the element is deformed elastically and is about to yield. Since J_3' changes sign with a reversal of stress it follows that the function ϕ in equation [2] must be an even function of J_3' whilst a function of J_2' satisfies the required condition.

The quadratic invariant of the deviator stress tensor, σ'_{ij}, namely

$$J'_2 = -(\sigma'_1\sigma'_2 + \sigma'_2\sigma'_3 + \sigma'_3\sigma'_1) = [(\sigma'_1)^2 + (\sigma'_2)^2 + (\sigma'_3)^2]/2$$

can be restated as

$$J'_2 = [(\sigma'_1 - \sigma'_2)^2 + (\sigma'_2 - \sigma'_3)^2 + (\sigma'_3 - \sigma'_1)^2 + 2(\sigma'_1\sigma'_2 + \sigma'_2\sigma'_3 + \sigma'_3\sigma'_1)]/4$$

However

$$2(\sigma'_1\sigma'_2 + \sigma'_2\sigma'_3 + \sigma'_3\sigma'_1) = (\sigma'_1 + \sigma'_2 + \sigma'_3)^2 - [(\sigma'_1)^2 + (\sigma'_2)^2 + (\sigma'_3)^2]$$

Therefore

$$(\sigma'_1)^2 + (\sigma'_2)^2 + (\sigma'_3)^2 = [(\sigma'_1 - \sigma'_2)^2 + (\sigma'_2 - \sigma'_3)^2 + (\sigma'_3 - \sigma'_1)^2 + (\sigma'_1 + \sigma'_2 + \sigma'_3)^2 - [(\sigma'_1)^2 + (\sigma'_2)^2 + (\sigma'_3)^2]]/2$$

and since $\sigma'_1 + \sigma'_2 + \sigma'_3 = J'_1 = 0$

$$3[(\sigma'_1)^2 + (\sigma'_2)^2 + (\sigma'_3)^2]/2 = [(\sigma'_1 - \sigma'_2)^2 + (\sigma'_2 - \sigma'_3)^2 + (\sigma'_3 - \sigma'_1)^2]/2$$

or

$$(\sigma'_1)^2 + (\sigma'_2)^2 + (\sigma'_3)^2 = [(\sigma'_1 - \sigma'_2)^2 + (\sigma'_2 - \sigma'_3)^2 + (\sigma'_3 - \sigma'_1)^2]/3$$

Hence

$$J_2' = [(\sigma_1' - \sigma_2')^2 + (\sigma_2' - \sigma_3')^2 + (\sigma_3' - \sigma_1')^2] / 6 \qquad [3]$$

If the values $\sigma_1' = \sigma_1 - \sigma_m$

$\sigma_2' = \sigma_2 - \sigma_m$

$\sigma_3' = \sigma_3 - \sigma_m$

are substituted into equation [3] then J_2' can be expressed in terms of the principle stresses as

$$J_2' = [(\sigma_1 - \sigma_2)^2 + (\sigma_2 - \sigma_3)^2 + (\sigma_3 - \sigma_1)^2] / 6$$

or in terms of the components of the stress tensor σ_{ij} , as

$$J_2' = [(\sigma_x - \sigma_y)^2 + (\sigma_y - \sigma_z)^2 + (\sigma_z - \sigma_x)^2]/6 + (\tau_{xy}^2 + \tau_{yz}^2 + \tau_{zx}^2)$$

2.2. Von Mises Yield Criterion

It was suggested by von Mises, in 1913, that quadratic invariant of the deviator stress tensor, J_2', should be considered as a yield criterion. Provided that J_2' is less than a characteristic value of the material, k^2, the material does not yield and the deformation is elastic. If no strain hardening occurs then J_2' can never exceed the value k^2 when the material yields.

Hence $J_2' < k^2$ during elastic deformation

and $J_2' = k^2$ at yield.

The von Mises yield criterion in terms of the components of the stress tensor, σ_{ij}, then becomes

$$J_2' = [(\sigma_x - \sigma_y)^2 + (\sigma_y - \sigma_z)^2 + (\sigma_z - \sigma_x)^2]/6 + (\tau_{xy}^2 + \tau_{yz}^2 + \tau_{zx}^2) = k^2$$

or in terms of the principle stresses

$$J_2' = [(\sigma_1 - \sigma_2)^2 + (\sigma_2 - \sigma_3)^2 + (\sigma_3 - \sigma_1)^2]/6 = k^2 \qquad [4]$$

The characteristic value, k, of the material can be evaluated by means of a uniaxial tensile test when the material is just yielding. Then $\sigma_1 = Y$ which is the uniaxial yield stress of the material, $\sigma_2 = \sigma_3 = 0$ and k is the yield stress in pure shear.

Substituting these values into equation [4] produces

$$[(Y - 0)^2 + 0 + (0 - Y)^2] = 6k^2$$

$$2Y^2 = 6k^2$$

$$k = Y/\sqrt{3}$$

and the yield stress in pure shear is $1/\sqrt{3}$ times the yield stress in uniaxial tension according to the von Mises yield criterion.

Equation [4] was also proposed independently by Huber (2) in 1904 and apparently by Maxwell in a letter to Kelvin as early as 1856. The von Mises yield criterion was further interprated by Hencky to mean that yielding commenced when the shear strain energy attained a critical value corresponding to yielding in uniaxial tension.

2.3. Tresca Yield Criterion

Tresca suggested, in 1864, that yielding occurs when the maximum value of the extremum shear stresses in the material attains a critical value. The extremum shear stresses (5) are given as

$$\tau_1 = \pm \frac{1}{2} (\sigma_2 - \sigma_3)$$

$$\tau_2 = \pm \frac{1}{2} (\sigma_1 - \sigma_3)$$

$$\tau_3 = \pm \frac{1}{2} (\sigma_1 - \sigma_2)$$

which are usually refered to as principle shear stresses. If σ_1 is the algebraic maximum principle stress, σ_3 the algebraic minimum priciple stress and σ_2 the intermediate principle stress such that $\sigma_1 > \sigma_2 > \sigma_3$, then the maximum value of shear stress designate τ_{max} is given by

$$\tau_{max} = \tau_2 = \pm \frac{1}{2} (\sigma_1 - \sigma_3)$$

It will then be seen that the maximum shear stress, τ_{max}, acts on the plane which bisects the angle between the planes of maximum and minimum principle stresses and is equal in magnitude to half the difference between these principle stresses. The Tresca yield criterion requires the maximum and minimum principle stresses to be known in advance.

For yielding in uniaxial tension when $\sigma_1 = Y$, $\sigma_2 = \sigma_3 = 0$

$$\sigma_1 - \sigma_3 = Y \qquad [5]$$

For pure shear, $\sigma_1 = -\sigma_3 = k$ and $\sigma_2 = 0$. Substituting these values into equation [5] produces

$$k - (-k) = Y$$

$$k = Y/2$$

That is, the yield stress in pure shear is half the yield stress in uniaxial tension according to the Tresca yield criterion.

Both the von Mises yield criterion and the Tresca yield criterion are used in solving plastic metal forming problems. Both are independent of hydrostatic stress and only depend on the components of deviator stress. The von Mises yield criterion is regarded as isotropic because each of the nine components of deviator stress has the same effect in the yield expression.

However, the Tresca yield criterion is uneffected by the intermediate principle stress σ_2. This implies that σ_2 can vary between a maximum value of $\sigma_2 = \sigma_1$ and a minimum value of $\sigma_2 = \sigma_3$ without affecting the criterion expressed by J_2'.

The von Mises yield criterion usually provides a better correlation, but not always, with the experimental data for engineering metals than does the Tresca yield criterion. The relative magnitudes of the principle stresses must be known, a priori, for application of the Tresca yield criterion. If the relative magnitudes of the principle stresses are known then the Tresca yield criterion is easier to apply and leads to simplicity in mathematical derivation.

2.4. Experimental Verification of Yield Criteria

The most common type of test specimen which has been used to experimentally investigate the yield criteria is a thin-walled tube subjected to combined stress. Thin-walled tube was used for this reason by Lode at the first time in 1926. The combined stress state can be achieved, for example, by subjecting the tube simultaneously to a couple C, an axial force F and an internal hydrostatic pressure p. By varying these parameters it is then possible to obtain different stress combinations which result in different magnitudes of principle stress and different principle stress directions. However, assume the thin-walled tube shown in figure 4 (a) to be subjected to a couple C, which produces elastic deformation, and then a tensile axial force F to be applied so as to just cause yielding. The angle of twist and the varying values of axial extension of the tube are noted as the tensile axial force increases. Yielding is assumed to have occured when the axial strain noticeably increases as discerned from an equivalent true stress, $\bar{\sigma}$ -equivalent natural strain, $\bar{\varepsilon}$ characteristic curve for the test material of the type presented in figure 4 (b).

For an element of the tube wall at the point P, the tensile axial stress is σ and the shear stress τ . Since the tube is thin walled the shear stress distribution across the wall can be assumed to be sensibly constant so that the shear stress τ is constant.

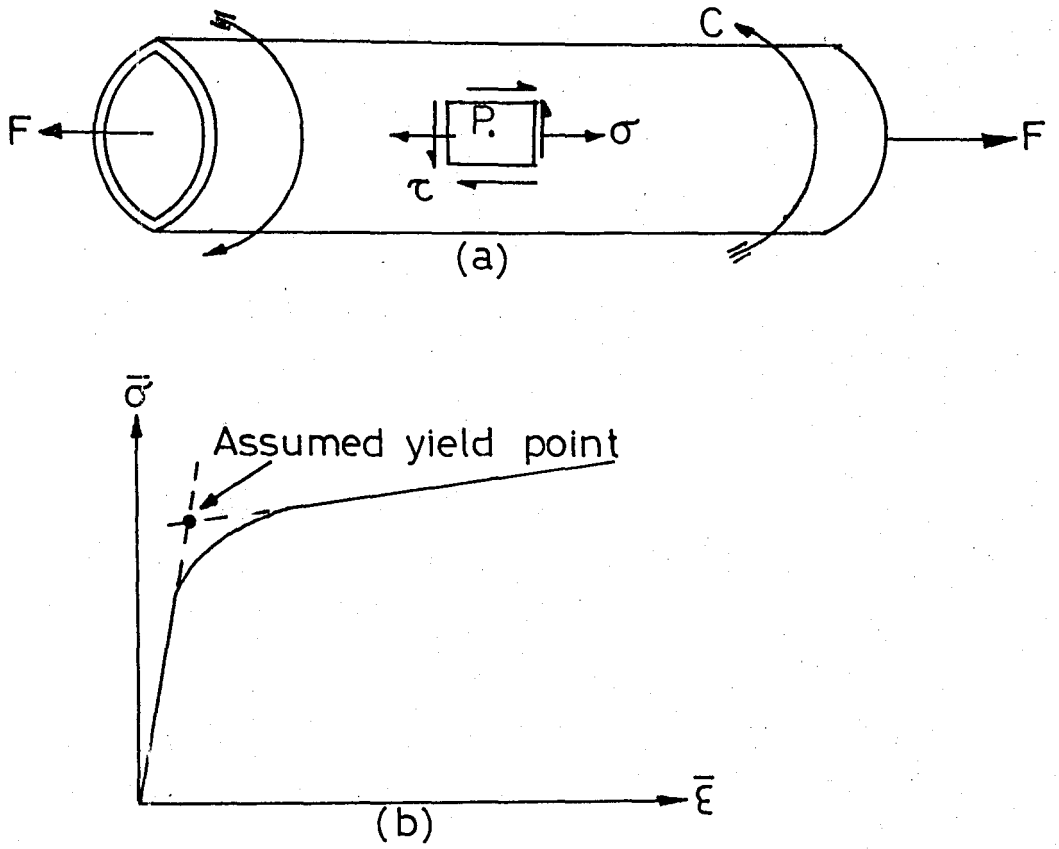

Figure 4. (a) Thin-walled tube subjected to a pure couple C and an axial force F showing the stress state at a point P; (b) Equivalent true stress, $\bar{\sigma}$ - equivalent natural strain, $\bar{\varepsilon}$ characteristic curve for the test material.(5)

The principle stresses at the point P in the tube wall at any instant are

$$\sigma_1 = (\sigma/2) + [(\sigma^2/4) + \tau^2]^{1/2}$$

$$\sigma_2 = (\sigma/2) - [(\sigma^2/4) + \tau^2]^{1/2}$$

$$\sigma_3 = 0$$

Therefore $$\sigma_1 - \sigma_2 = (\sigma^2 + 4\tau^2)^{1/2} \qquad [6]$$

and $$(\sigma_1 - \sigma_2)^2 + (\sigma_2 - \sigma_3)^2 + (\sigma_3 - \sigma_1)^2 = 2\sigma^2 + 6\tau^2 \qquad [7]$$

By using [6] the Tresca yield criterion predicts

$$\left(\frac{\sigma}{Y}\right)^2 + 4\left(\frac{\tau}{Y}\right)^2 = 1 \qquad [8]$$

and using equation [7] the von Mises yield criterion predicts

$$2\sigma^2 + 6\tau^2 = 2Y^2$$

or $$(\sigma/Y)^2 + 3(\tau/Y)^2 = 1 \qquad [9]$$

where Y is the uniaxial yield stress of the tube metal in tension.

Both equations [8] and [9] plot as ellipses in the σ-τ plane and in dimentionless form represented in figure 5.

Experimental data obtained in this manner are found to plot between the two ellipses although generally closer to the von Mises ellipse. These deviations from the theoretical predictions are usually partially attributed to a degree of anisotropy of the specimen material and to experimental inaccuracy.

The classical experimental work of this kind was performed in 1931 by Taylor and Quinney which was intended to solve this problem. They used copper, mild steel and aluminum thin-walled tubes, which were said to be very nearly isotropic, and tested them in combined tension and torsion. However, they also observed similar deviations from the theoretical curves and concluded that these discrepancies were real and could not be attributed to experimental error or anisotropy of the specimen material.

Similar results were obtained earlier, for example, by Lode (5) in 1926, by Ros and Einchinger in 1929 and, in 1953, by Siebel who employed combined bending and torsion. Details of other tests of a similar nature can be found in the literature and an extensive survey of the literature concerned with this topic up to about 1976 was presented by Hecker (3).

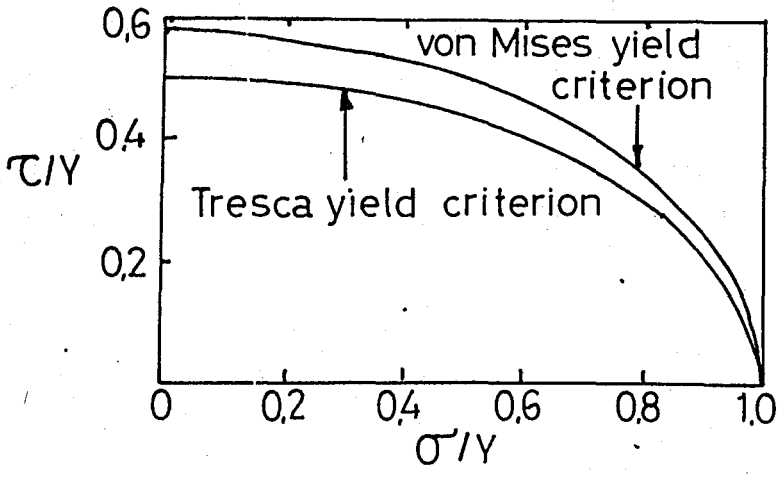

Figure 5. the Tresca and von Mises yield criteria represented in dimensionless (σ/Y)-(τ/Y) plane for a biaxial stress state.

2.5. Bauschinger Effect

In general, the effect of plastically deforming a metal at room temperature is to increase to further deformation by virtue of strain hardening. This provides a means of improving the strength and hardness of a component and there are many applications where this property is utilised to advantage.

When a metal is stressed to produce plastic deformation and then unloaded, residual stresses on a microscopic scale remain due mainly to the different states of stress existing in the differently oriented crystals before unloading occurs. If a reversal of stress now occurs then such residual stresses could be expected to have some influence on plastic yielding. Suppose that a specimen is subjected to a uniaxial tensile stress which exceeds the initial tensile yield stress, + Y, so as to produce plastic deformation, corresponding to point A in figure 6 and then unloaded to point B. Neglecting hysteresis, the unloading

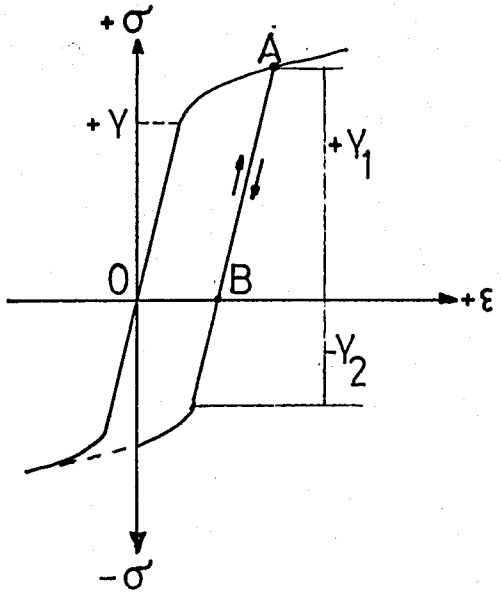

Figure 6. The Bauschinger effect [5].

will occur elastically and an inrecoverable plastic deformation results. On reloading in tension, the reloading path follows the elastic line BA and the subsequent tensile yield stress, $+Y_1$, is greather than the initial yield stress $+Y$. If, however the specimen after unloading to the point B is now subjected to uniaxial compression it is observed that, because of the residual stresses present on unloading, yielding of the specimen as a whole occurs at a reduced magnitude of stress, $-Y_2$, and it is possible that this may even be lower than the initial tensile yield stress, $+Y$.

This phenomenon is known as Bauschinger effect and is present whenever a reversal of stress occurs. Since the effect is known to be absent from single crystals of pure metals it is believed to be attributable to a particular kind of residual stress influenced by the grain boundaries. It would therefore appear that components which are to be, say, subject to tension in service should not be strain-hardened by compressive loading.

The residual stresses and consequently the Bauschinger effect can be removed by a low temperature heat treatment. In contrast, to change the preffered orientation of crystals responsible for the anisotropy of a metal it is necessary for the heat treatment to be carried out above the recrystallizatio temperature.

III. EXPERIMENTS

Before starting the experiments, the machine was calibrated carefully. The calibration was made before mounting the specimen to the machine. For calibration, one must put the tension and torsion arms of the machine to the horizontal position. This was made by adding small amounts of weight to the arms. When ever the arms were horizontal, the machine was able to operate by putting a few grams of weight.

After calibration, the first specimen was mounted to the machine. The strain gages were combined to the channel selector and then to the indicator.

After all these preliminary works, the experimentation was started. The test specimen was subjected to pure tension, pure torsion, shear probe and proportional loading. Probes of added shear stress at constant axial stress is called shear probe. Proportional loading is defined as probing along radial paths from the origin ($\tau = k\sigma$) . All types of loading are shown in Fig.7

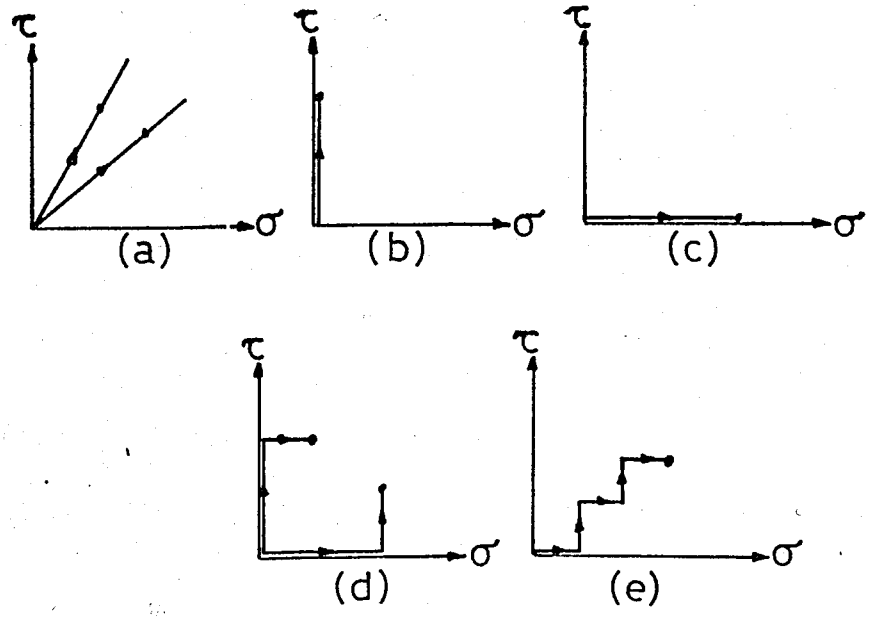

Fig.7. Types of loading.

a. Proportional Loading ($\tau = k.\sigma$)

b. Pure torsion

c. Pure tension

d. Shear probe

e. Small path loading

In order to obtain the points on the yielding curve, σ-ε curve was plotted for each point. For better explanation, obtaining of the point(1) on the initial yield curve (Fig.28) of the annealed aluminum is shown in figure 8.

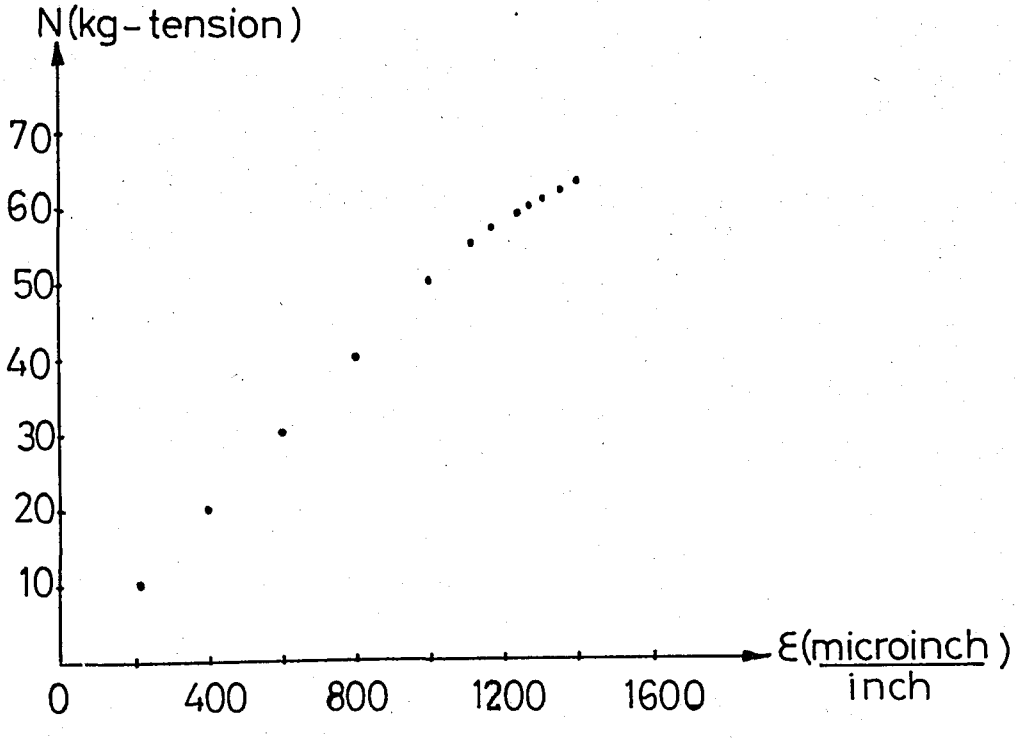

Figure 8. σ - ε curve of point (1) of annealed aluminum on the initial yield curve.

This is a pure tension loading. It was obtained by adding small increments of load to the temsion arm. Stress increments are seen in figure 8.

Loading program for this point was plotted in figure 9.

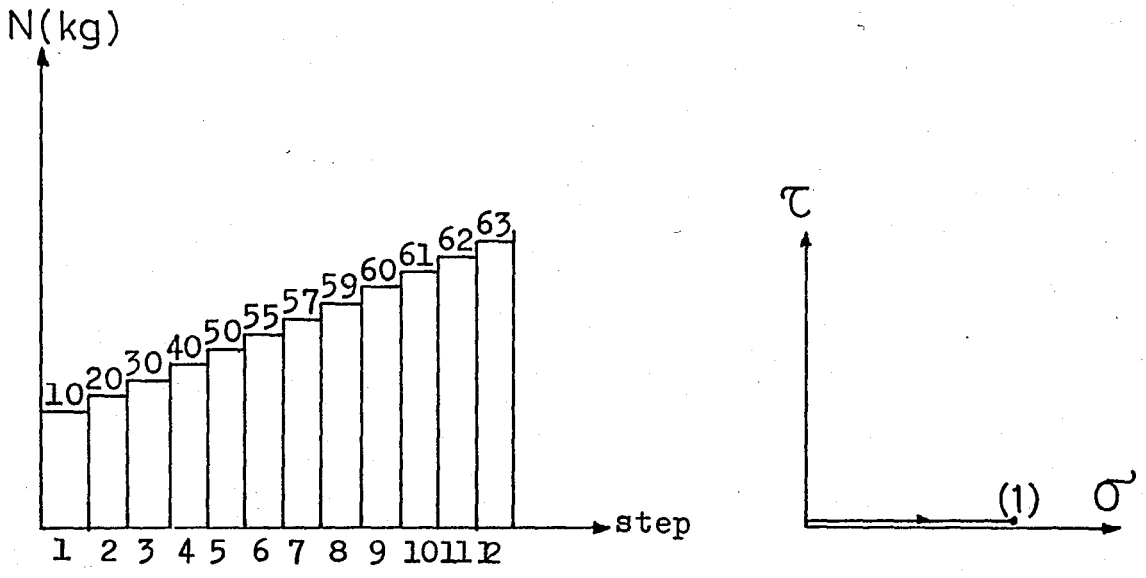

Figure 9. Loading program of the point(1) on the initial yield curve of the annealed aluminum specimen.

The curve in figure 8 was linear up to 60 kg of load. Thereafter it began to deflect from linearity. Deflection means that the plastic deformation is started. Whenever small measurable plastic deformation was reached, the loading was stopped. For this case 63 kg tension load can be accepted as the beginning of yielding. The yielding stress of point(1) corresponding to 63 kg was calculated as 8.96 kg/mm^2.

When the yielding point is reched, it should be unloaded quickly. Because, after yielding,strain increments increase rapidly and specimen undergoes large plastic deformation.

In order to find the amount of permanent plastic deformation, the strains read from the indicator before loading were subtracted from tne strains read after unloading. By this way ε_A , ε_{45} and ε_C were found. These values were used for controlling the normality condition.

The same procedure was followed for other points. For the initial yield curve of the annealed Al, 9 points were found and then the yield curve was plotted (Fig.28).

3.1. Stress Calculation

Thin walled tubes ($tw \ll r$) are the most suitable type of specimen in which the stress is constant and is computable directly from the applied load witnout any referance to the properties of the material.

Consider axial tension alone N (figure 10) applied to the specimen. The central region is in a state of homogeneous stress (uniform).

$$\tau = \sigma_r = \sigma_c = 0 \quad , \quad \sigma_a = \frac{N}{\pi(R^2 - r^2)}$$

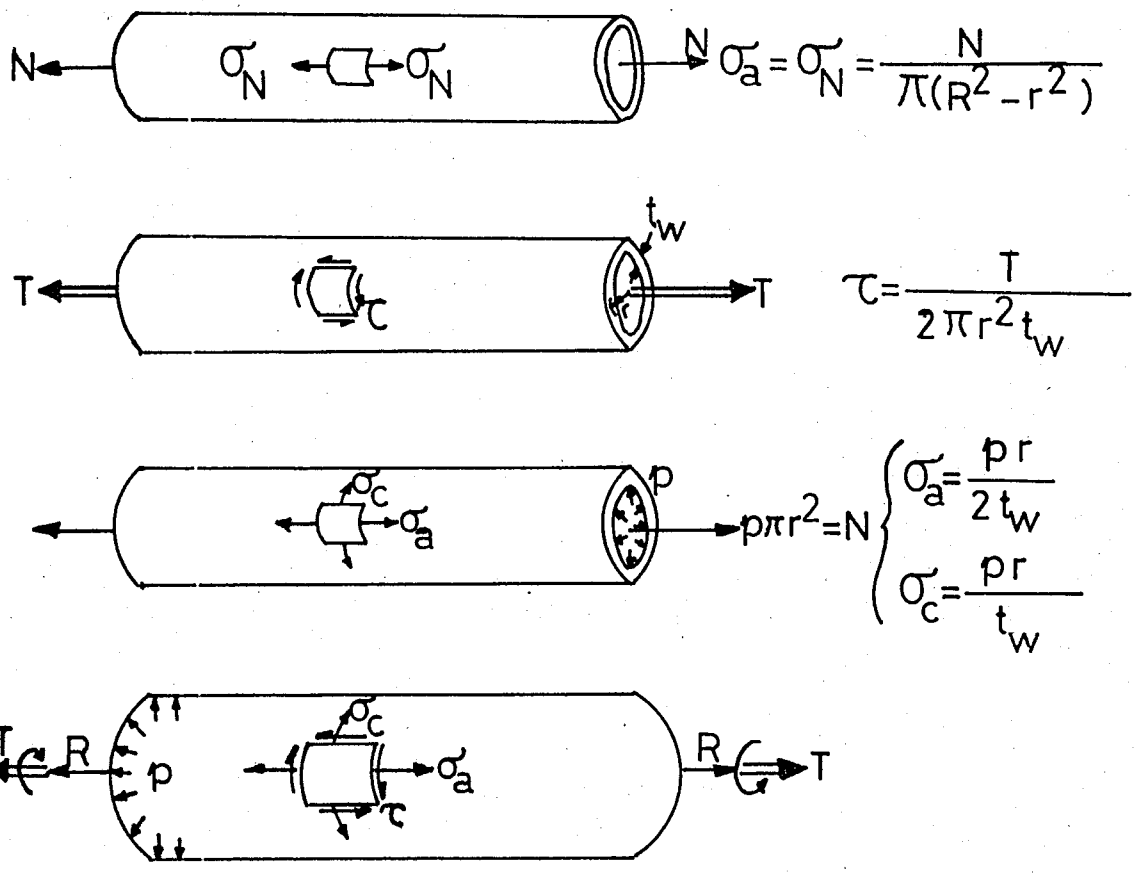

$$\sigma_a = \frac{N}{\pi(R^2 - r^2)} = \frac{pr}{2t_w} = \frac{R}{\pi(R^2 - r^2)}$$

$$\sigma_c = \frac{pr}{t_w}$$

$$\tau = \frac{T}{2\pi r^2 t_w}$$

Figure 10. Thin-walled circular tube under combined loading.(4)

Consider the specimen as an axisymmetric thin walled tube and under almost homogeneous stress,

$$\tau = T/2\pi r^2 t_w \qquad \sigma_a = \sigma_c = \sigma_r = 0$$

due to the twisting moment T alone (Fig.10).

Interior pressure p alone gives $\sigma_a = pr/2t_w$, $\sigma_c = pr/t_w$, $\tau = 0$ and negligible σ_r.

Any combination of N, T and p will produce an almost homogeneous state of plane stress σ_a, σ_c, τ. The total stress is the sum of stresses which would be caused by each load acting alone.

3.2. Testing Machine

The machine (7) used in this study has been designed for tests of high sensitivity on tubular specimens subjected to combinations of tension, torsion and internal pressure at various temperatures. This machine also minimizes the influence of one loading system on the other. Load capacity is 6000 kgs in tension, 3500 kg-cm in torsion, and 100 kg/cm^2 internal pressure. Extensions of 1 inch or more and rotations of 150 deg can be accomodoted without interference between loading systems. A low-friction hydraulic thrust bearing and

knife-edge pivots provide nearly frictionless loading. Either constant load or constant strain tests may be performed. A proportional loading device permits applying the load at a constant ratio of tension to torsion followed by excursions along another constant ratio of increments of tension and torsion. Torsion may be applied in either direction continuously through zero.

Equipment of the type described is needed to permit tests of sufficient accuracy and versatility to provide the information desired in number of important problems especially in verifying present theory of stress-strain-time-temperature relations under multiaxial stresses for metals, plastics, and composite materials. Some of the experiments, especially yield surface determinations in plasticity experiments, require superimposing small changes in tension, torsion, or internal pressure on a specimen already heavily loaded. Determinations of the resulting small changes in strain requires a high degree of sensitivity of the loading and strain measuring systems. The accuracy of calibration required is not greather than usually available.

The machine consists of four columns to which levers, pulleys, and other devices are attached as shown in Figure 11. The entire assembly is mounted on a concrete block. Tension up to 6000 kgs can be applied to a tubular specimen by means of 20 to 1 lever and weights. Torque up to 3500 kg-cm is applied to each end of the specimen by means of 25.4 cm diameter drums which are acted on by steel tapes passing over a system of pulleys as shown diagramatically in Fig. 12. The torque load is applied by means of a

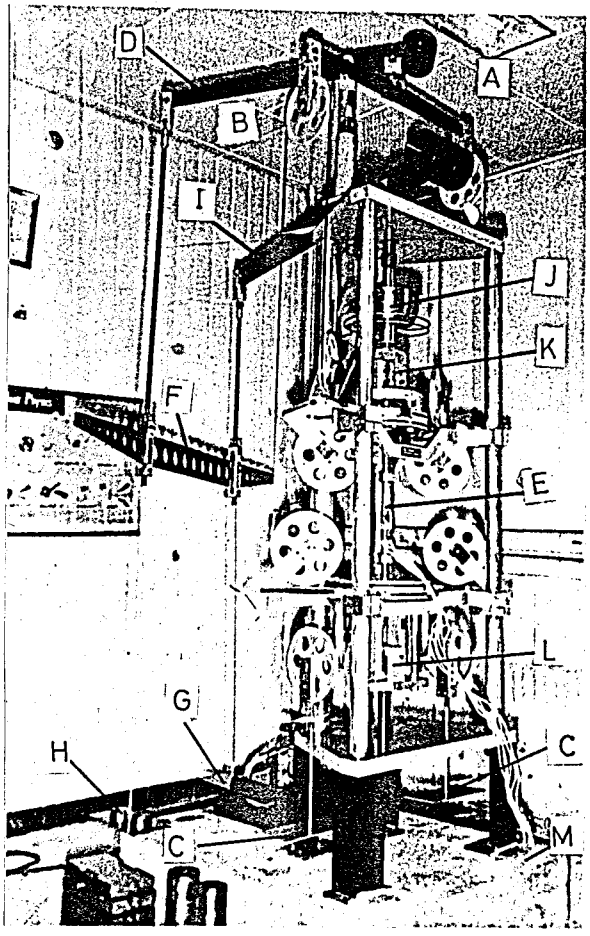

Fig. 11. Machine for combined tension, torsion and internal pressure tests of thin-walled tubes.

lever and weights in such a way that torque may be produced in either sense. Steady fluid pressure may be applied inside the tube for perssures up to 100 kg/cm^2 and maintained constant by means of a dead weight gage tester with a continuously rotating piston.

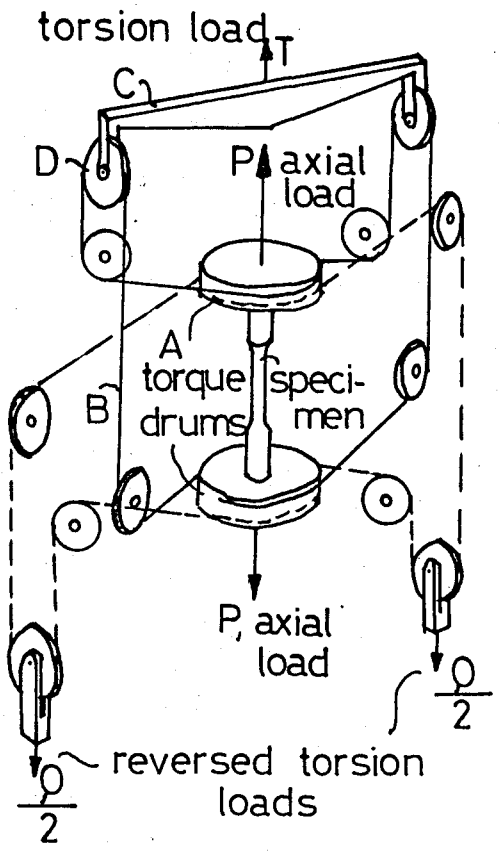

Figure 12. Schematic diagram of torque applying pulley system.(7)

3.2.1. Axial Loading

a. Knife-Edges

To ensure axial loading, each end of the specimen was connected to its respective pull rod by a universal joint. Each such joint consisted of two yokes (A, Fig. 13) and a pair of knife-edges B intersecting at right angles. It was possible to move each knife-edge assembly transverse to pull rod by means of adjusting screws C. The axis of the specimen and the loading axes of the testing machine could be made to coincide. Adjustable stops

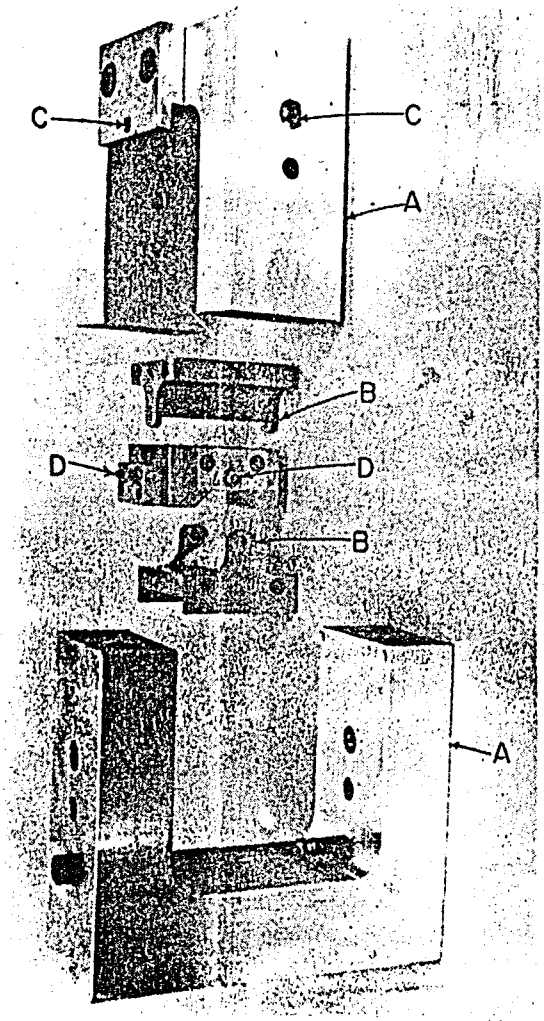

Fig. 13. Exploded view of crossed-knife edges and yokes. (7)

D were provided to prevent shifting of the knife edges in their seats after adjustment had been made.

b. Hydraulic Thrust Bearing

One of the most difficult problems to solve was that of minimizing the resistance imposed by the tension loading structure when twisting couples were applied. In this machine a hydraulic thrust bearing was accordingly incorporated. The cross section of this bearing is shown in Fig. 14. A piston (A,Fig.14) mounted within a cylinder B

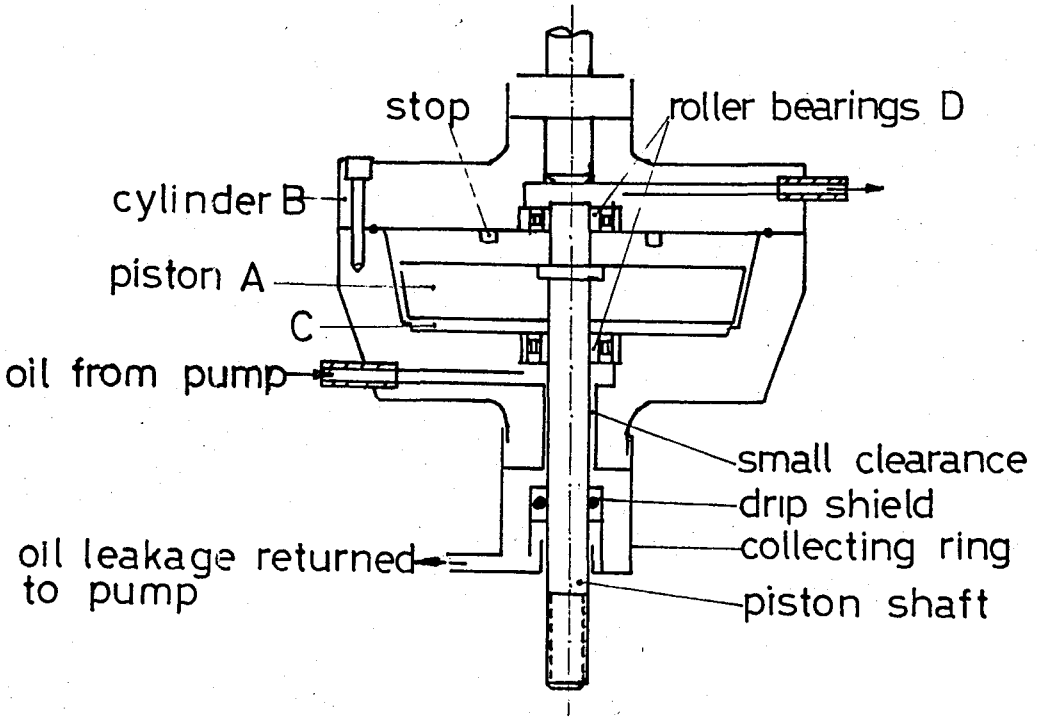

Figure 14. Cross-section of hydraulic thrust bearing. (7)

was supported by oil pumped by a pump into the cavity C under the piston at the rate required to keep the piston elevated slightly above the seat. Oil was permitted to flow through an annular space between the piston and the cylinder. The flow was regulated by the output of the adjustable displacement pump. The required resistance to flow in annular ring was self-adjusting by means of a taper built into the cylinder wall and piston. To prevent unbalanced lateral pressures in the annular ring of oil from forcing the piston againts the piston wall,

the piston shaft was mounted on roller bearings D. These permitted axial movement and introduced only small frictional torques because the bearings operated under essentially no load. It was found that the torque reaction of the hydraulic bearing as measured by a sensitive torque bar was about 0,08 kg-cm under an axial thrust of 1800 kg when the rate of rotation of the bearing was slow. Viscous friction of the oil in the annular space between the piston and cylinder wall introduced a larger reaction at higher rates of rotation.

3.2.2. Torsion Loading

The torsion loading was designed to ensure as nearly as possible that equal colinear torque vectors were applied at each end of the specimen. To accomplish this, torque was applied to the pull rod attached to each end of the specimen by means of drums (A, Fig.15;A, Fig.12) and steel tapes (B,Fig.15; B,Fig.12) passing over a system of pulleys from one drum to the other as shown diagramatically in Fig.12. The force in the tapes B was developed by applying weights to the end of an overhead lever of 4 to 1 ratio on an equalizing lever (A,Fig.11, C,Fig.12) supporting pulleys (B,Fig.11; D,Fig.12). In order to minimize friction, all pulleys were mounted on knife-edge bearings resting against hardened seats and rigid

supporting blucks. The angular rotation permissible with the knife-edges limited the over-all angle of twist of the specimen. Accordingly, ball bearings were also incorparated in the pulleys and the knife-edges were made a part of the spindle carrying the bearings. Thus adjustments in knife edge position could be made during a test, and in the event of overtravel of the knife-edge the ball bearings

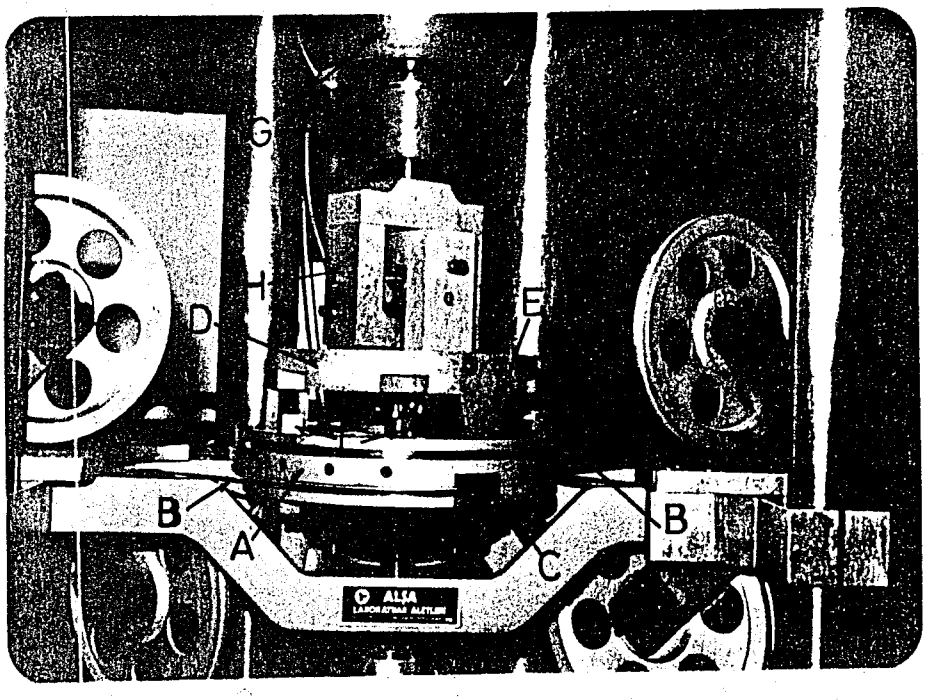

Fig.15. Detail of hydraulic thrust bearing, G, crossed knife-edges, H, upper torque drum, A, and torque transfer system, D,E,F.

permitted further rotation. Also in order to minimize friction and ensure accurate control over the direction of the torque vectors, the tapes were placed in grooves having tapered sides both in the drums and

the pulleys. In order to minimize the forces resulting from the bending the tapes, the tapes were made as thin as possible (0,25 mm). This required special attention to the clamps at the ends of the tapes so that full strength of the tapes could be employed. The clamps consisted of a cap (C,Fig.15) fastened by screws to the drum and containing a tapered wedge located so that the band passed under and over the wedge in such a way that a pull on the band tended to increase the holding power of the clamp.

Reverse torque was made possible by adding a seperate system of bands and pulleys as shown in Fig.12, producing torque in the opposite sense to the first set, and hanging dead weights (C,Fig.11)from each of the free pulleys. Thus torque in one sense was applied by force T (Fig.12), and torque in reverse sense by equal force Q/2 (Fig.12). In operation the weights (C,Fig.11) were initially balanced by weights on the lever (D,Fig.11) so that resultant torque on the lever produced a twisting moment of one sense, whereas remaining some of the balancing weight from the lever caused a twisting moment of opposite sense.

3.2.3. Interfrence Between Loadings

In order to permit large elongations of the test specimen without interference between the tensile loading and torsional loading, a mechanism was

incorporated, as shown in Fig.15, to permit the upper torque drum (A,Fig.15) to remain in one horizontal plane, in spite of vertical movement of the upper pulling head (D,Fig.15). This was necessary in order to prevent vertical displacement of the torsion bands (B,Fig.15) from introducing axial thrust during large tensile deformations. The objective was accomplished by supporting the torsion drum on an air thrust bearing and transmitting the torque through three large hardened rollers to brackets (E,Fig.15) attached to the upper pulling head. Each of the three hardened rollers lay between pairs of hardened guides (F,Fig.15) so that torque could be transmitted in either direction. The large-diameter rollers and hardened guides were employed in order to minimize axial friction resulting from torque. The air thrust bearing permitted the torque drum to shift laterally to prevent lateral restraint being applied to the specimen.

3.2.4. Proportional Loading and Variable Principle-Stress Ratios

A feature was incorporated in the design of this equipment which permits a given proportion of tension and torsion to be applied in increments by merely adding weight to a scale pan. Proportional loading method is explained in Fig.16. This was arranged by providing a beam (F,Fig.11) suspended at one

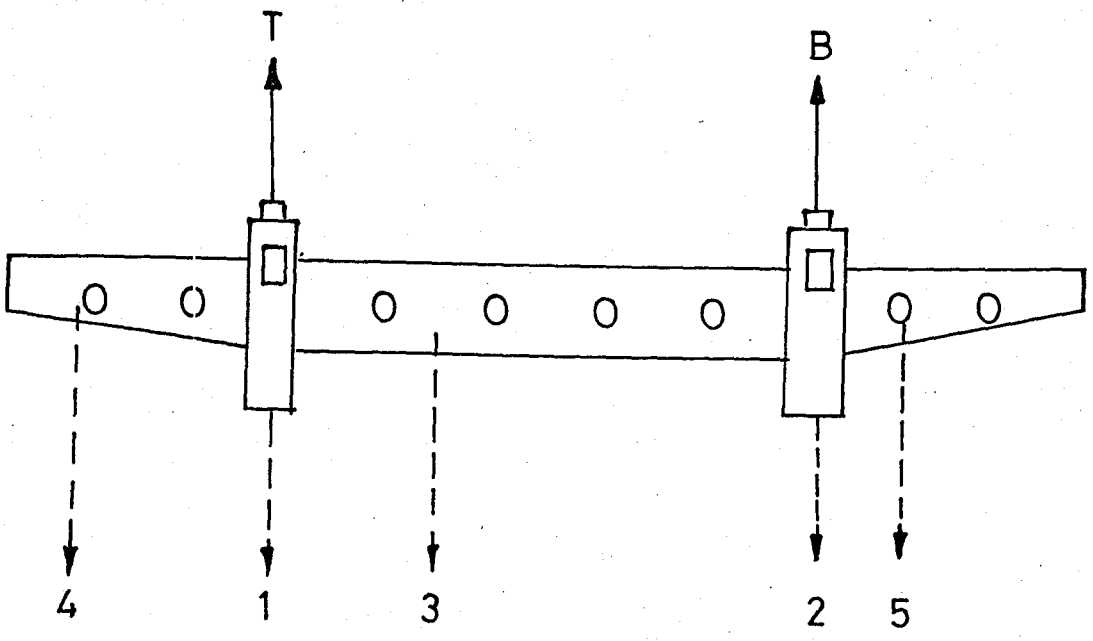

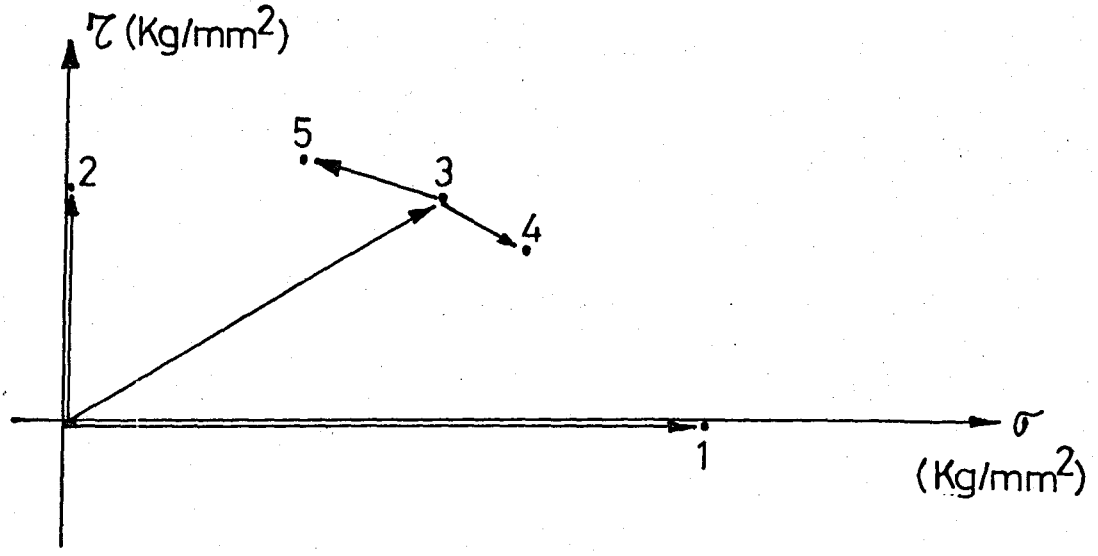

Figure 16. Proportional loading beam (4).

Loading points	Loading types
1	pure tension
2	pure torsion
3	proportional loading

point from the loading end of the tensile lever and suspended at another point from the loading end of the torque lever. If loads were applied to the beam between the tensile and torsion suspension points, the tension and torsion would increase in the same proportion for each load increment. This is a positive ratio of tension to torsion. If loads were applied to a cantilever extension at either end of the beam, then one of the loads would be increased and the other decreased (a negative ratio of tension to torsion). Thus it was possible to increase the loads in a constant ratio of tension to torsion to any desired value and then to make additional changes in loading at another ratio of tension to torsion by applying additional loads at a different point on the beam. With the arrangement shown a limited range of negative ratios of tension to torsion could be achieved. The possible combinations were increased by the addition of another beam suspended at one point from the loading end of the torsion lever and suspended at another point from the counterweight end of the tension lever. The addition of a weight at a point between the suspension points of this beam caused an increase in torque and a decrease in tension.

In order to maintain high sensitivity of the system these beams were also equipped with knife-edge pivots

and the loads were applied to the beam through knife-edges. All knife-edges acting on a beam are on one line, so that the proportion of loads is not altered significantly by deviation of the beam from horizontal.

3.2.5. Internal Pressure

The test machine was designed not only to subject the specimen to combinations of tension and torsion but to internal pressure as well. Steady fluid pressure may be applied inside the tube for pressures up to 100 kg/cm^2 through a hole in the lower pull rod which can be designed for this purposes. O-Rings should be provided to seal the ends of the specimen for tests.

Pressure was maintained constant by means of the aparatus shown in Fig.17. This aparatus was designed after the testing machine as a dead weight type tester. This aparatus was not used for the present investigation. The test specimen was under combined tension and torsion. The interior pressure was not applied.

The aparatus consisted of an injector pump element as a dead weight type of hydraulic gage tester, (A,Fig.17). It employes a free piston of 19 mm. diameter, which acted on the bottom by the test pressure and

loaded on at the top by the required force which is transmitted by means of a 5 to 1 lever and weights (C, B, Fig.17).

In order to prevent friction of the piston during vertical displacement of that, the lever was mounted on knife edge vearings resting againts hardened seats and rigid supporting blocks (D, Fig.17). It consisted

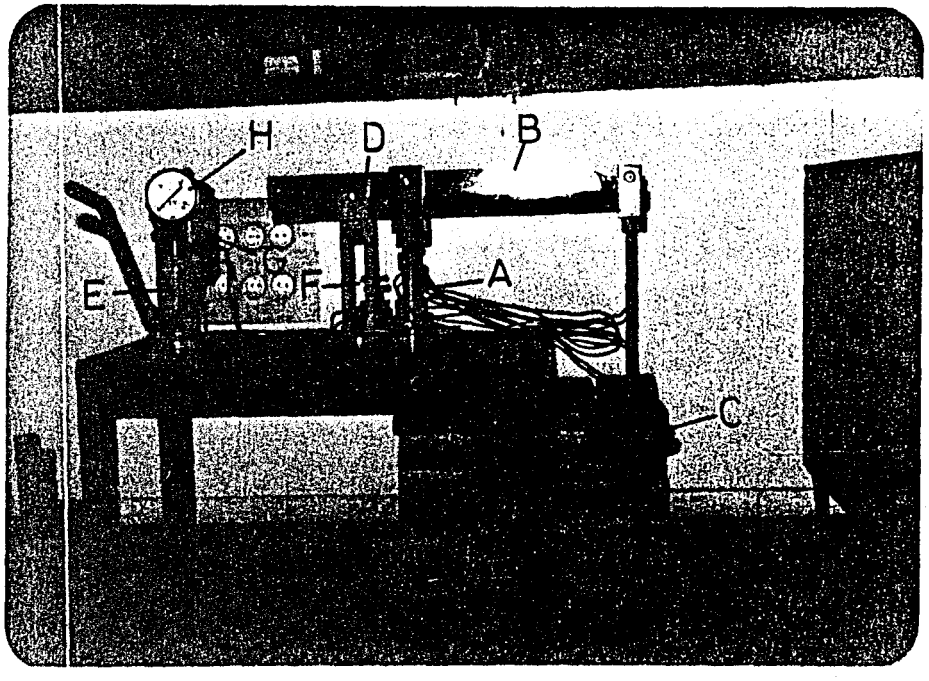

Figure 17. Constant internal pressure aparatus.

of a hand driven type haydraulic specimen after gaining a constant pressure by means of the piston. After having conduced the experiments, in order to emty the oil from inside of the specimen a vane is mounted on the hydraulic tube (F, Fig.17) which allow the oil back to the oil tank (G, Fig.17).

By adding necessary weights to the pan (C,Fig.17), it can be reached to the desired perssure. The pressure can be read from the manometer at the top of the pump (H,Fig.17).

3.2.6. Adjustments

In order to prevent a number of errors some inspection and adjustments were performed before starting the experiments.

Several potential errors were considered such that bending moments induced by the tensile load did not pass through the centroid of the cross section of a homogeneous specimen. Even if the specimen and pull rods are perfectly concentric their assembly contains several joints whose mating surfaces must be parallel within very small tolerances. Since such tolerances can not be achieved, there is need for the adjustable knife edges. They adjust passing the tensile load through the centroid of the cross section of the specimen.

If both torque vectors of the applied torques are not parallel with the longitudinal axis of the specimen they will have bendings as well as twisting components. If they are not parallel to each other, they will also require transverse forces to maintain equilibrium. In order to prevent the bending stresses

in this case, the torque-applying drums must be parallel to each other and perpendicular to the specimen.

Bending stresses may also be introduced by the twisting mechanism if the auxiliary pulleys are not in their optimum position. If they are not properly lined up in the horizontal plane, transverse forces will result.

To ensure this adjustments the strains were recorded from both left and right gages after the stress was applied and the knife-edges were adjusted untill a perfect alignment was achived.

3.2.7. Sensitivity

The sensitivity of the loading systems was determined after calibration of the machine by observing the minimum weight. The sensitivity was controlled under no load condition in the absence of specimen. The beginihg of the movement of loading systems was observed by putting dialgages under the longer sides of the levers where the displacement is greather. Under no load no specimen conditions, the axial system was sensitive to 2 gr and the torque system was sensitive to 10 gr at the pen ends of the systems.

3.3. Test Specimens

Five kinds of tubular specimens were machined from different kinds of materials. The material of the first specimen was AA 1100 and the composition of it is shown in table 2.

Table 2. The composition of the first specimen.

Elements	%
Cu	0.05-0.20
Fe + Si	1.0
Zn	0.1
Mn	0.05
Other	0.15
Balanced	98.5-99 Al

The second specimen was machined from a cast Al bar. The third and the fourth specimens were made up of ETİAL 60 aluminum bar stocks. A 60 mm diameter Al bar was extruded to 50 mm diameter. This extruded bar was used for the third specimen without any heat treatment. For the fourth specimen, the same extruded bar was taken and age hardenet at 180 ± 3°C for 6 hours. The third and the fourth specimens have the composition shown in table 3.

The fifth specimen was non-metallic. It was a polymer named polyethylene. It was bought as a pipe which has an insid diameter of 25 mm and outside diameter of 29 mm. The specimen was prepared from this material. The two ends of the specimen

Table 3. The composition of the third and fourth specimens.

Elements	%
Fe	0.35
Si	0.20-0.60
Cu	0.10
Mn	0.10
Mg	0.45-0.90
Zn	0.10
Ti	0.10
Cr	0.10
Others	0.15

were thickened by polyester. By this way the thickness of the ends of the specimen were increased from 2 mm to 12.5 mm. Polyester was mixed with Mek peroxide which hardens it and mixed with cobalt Naftenat in order to increase the speed of reaction. The ends of the polyethylene tube was strengthen by putting glass-fiber within the polyester. After then the specimen was machined by a lathe as seen in figure 19.b.

3.3.1. Heat Treatments

In order to get a softer product and to remove the effects of strain hardening a "stress relieve annealing" was accomplished to the first and second specimens. They were heated to 450± 5°C and held there for two hours. After then they were cooled to the room temperature by air cooling.

The third specimen (ETİAL-60) was not subjected to any heat treatment.

The fourth specimen (ETİAL-60) was not annealed but age hardened by heating to 180 ± 3°C and keeping there for six hours and air cooling.

3.3.2. The Specimen Geometry

The specimen geometry of the first four samples was a right circular cylinder (Fig.18) of nominal

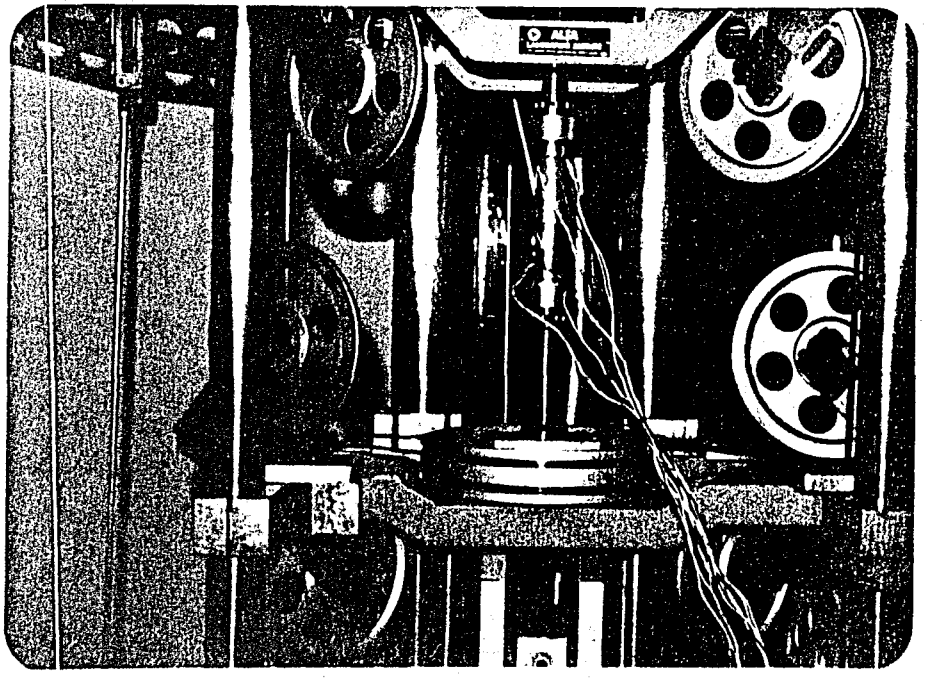

Figure 18. The specimen mounted on the machine.

dimensions of 29 mm outside diameter, 1.5 mm wall thickness, and tube length between flanges was approximately 110 mm. The diagram of these test specimens was shown in figure 19a. The fifth sample

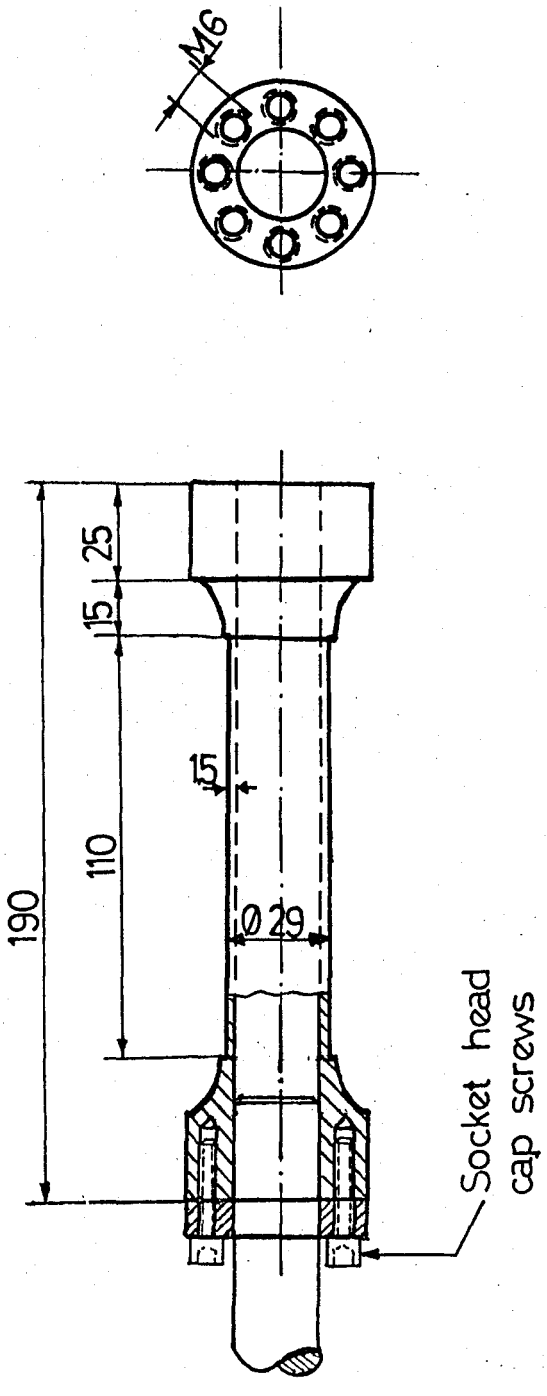

Figure19a. The geometry of aluminum samples.

which is polyethylene, has a different geometry. It is shown in Fig. 19b.

The wall thickness should be varied as required to accomplish the buckling requirements of each material and loading. The 1.5 mm wall thickness is sufficient for our case. Both inside and outside of the specimens were machined at the lathe. During machining the outer and inner surfaces and drilling the screw holes, kerosene was used for easy chipping.

In order to find the correct values of the stresses we needed to know the exact values of the wall thickness. For the measuring the exact values of the wall thicknesses, a steel bar was held by lathe. Two small steel spheres were mounted on the bar as shown in figure 20. Before putting the samples on the spheres, the top level of one of the spheres was measured by a comparator. Then the samples were put on the spheres from different points and wall thicknesses were measured. The results were tabulated and average wall thicknesses were found. In the tables the numbers 1,2,3 and 4 illustrate the circumferencial points and I, II and III longitudinal points on the samples. After the measurements, the wall thicknesses of the samples were found as below.

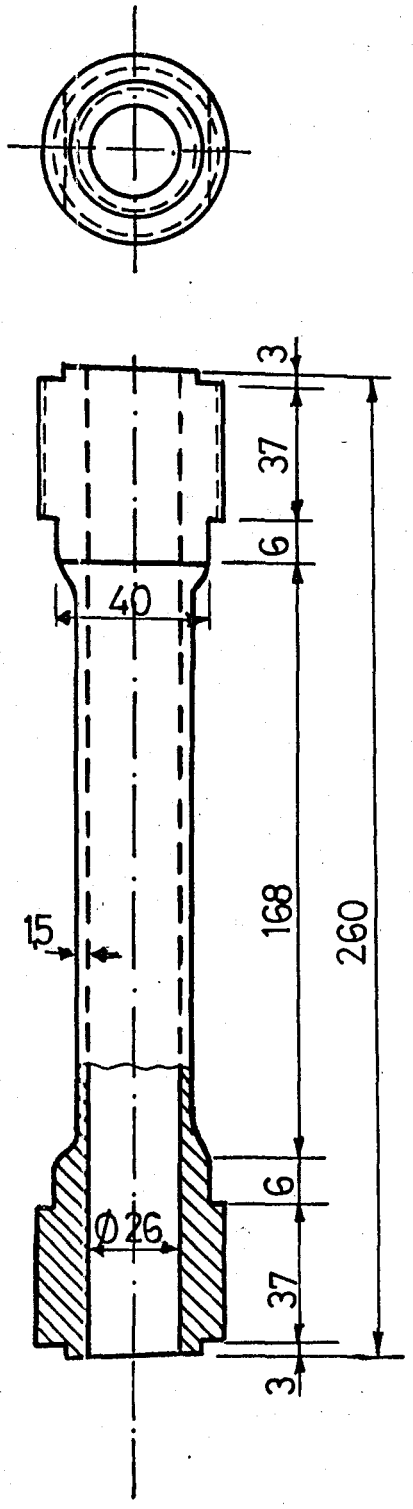

Figure 19b.The geometry of polyethylene sample.

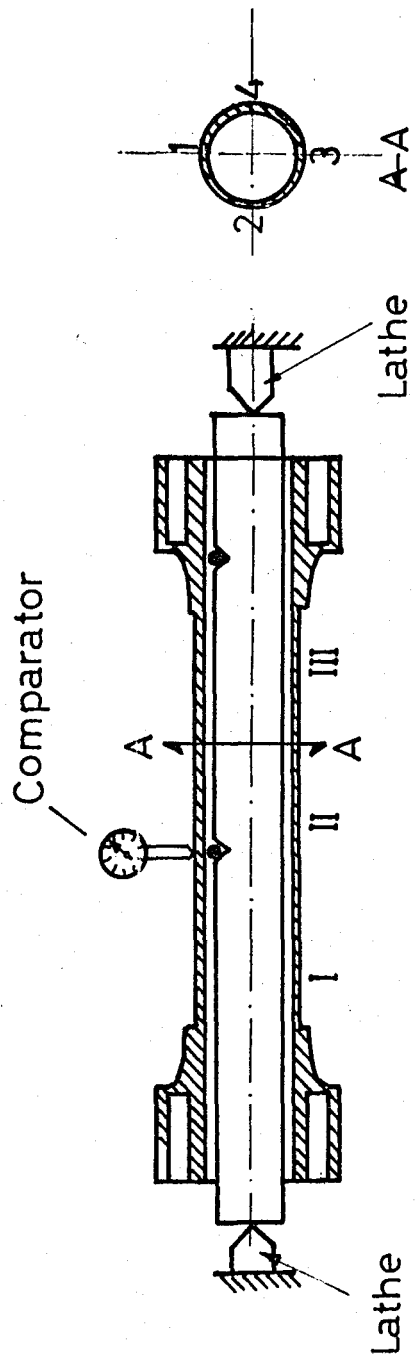

Figure 20. Finding the wall thickness of the specimen.

Table 4. The wall thickness readings of the annealed aluminum sample.

t,mm	I	II	III
1	1.62	1.65	1.67
2	1.58	1.59	1.59
3	1.60	1.62	1.65
4	1.59	1.63	1.60

$\bar{t} = 1.62$

Table 5. The wall thickness readings of the cast aluminum sample.

t,mm	I	II	III
1	1.95	1.81	1.78
2	2.00	1.92	1.84
3	1.95	1.92	1.90
4	1.90	1.85	1.82

$\bar{t} = 1.89$

Table 6.The wall thickness readings of the extruded ETİAL 60 sample.

t,mm	I	II	III
1	1.37	1.44	1.44
2	1.39	1.40	1.45
3	1.40	1.44	1.44
4	1.42	1.45	1.41

$\bar{t} = 1.42$

Table 7. The wall thickness readings of the age-hardened ETİAL-60 sample.

t,mm	I	II	III
1	1.39	1.43	1.43
2	1.40	1.42	1.42
3	1.42	1.42	1.45
4	1.40	1.42	1.42

$\bar{t} = 1.42$

Table 8. The wall thickness readings of the polyethylene sample.

t,mm	I	II	III
1	2.05	2.05	2.00
2	2.10	1.96	1.96
3	2.01	2.00	1.95
4	1.98	1.94	1.96

$\bar{t} = 2.00$

If the variation of the wall thickness along the sample axis is more than five percent, it should not be used. A new sample must be prepared.

The samples used in this study is summarized in table 9.

	Material	Heat Treatment	Wall Thickness(mm)
Sample-1	AA-1100	Annealed at 450 °C for 2 hrs and air cooled.	1.62
Sample-2	Cast Al	Annealed at 450 °C for 2 hrs and air cooled.	1.89
Sample-3	ETİAL-60	After extrusion no heat treated.	1.42
Sample-4	ETİAL-60	After extrusion age hardened at 180 ±5 °C for 6 hours.	1.42
Sample-5	Polyethylene	No heat treatment	2.00

Table 9. Summary of the samples used.

3.4. Strain Measurements

Two SR-4 type strain gage rosettes were applied to the outer surface of the specimen positioned 180° apart at mid lenght in location.(centered on the 110 mm gage length). They are referred to as left and right gages. These strain gages were attached to a chanel selector and the chanel selector was attached to the strain indicator. By this way we can read each strain easily. The gages were applied before the specimen had assembled on the testing machine. In order to stick the gages to the outer surface of the specimen, glue 404 was used. After sticking, one kilogram weight was hanged with a band as shown in figure 21 and waited for 24 hours in this position.

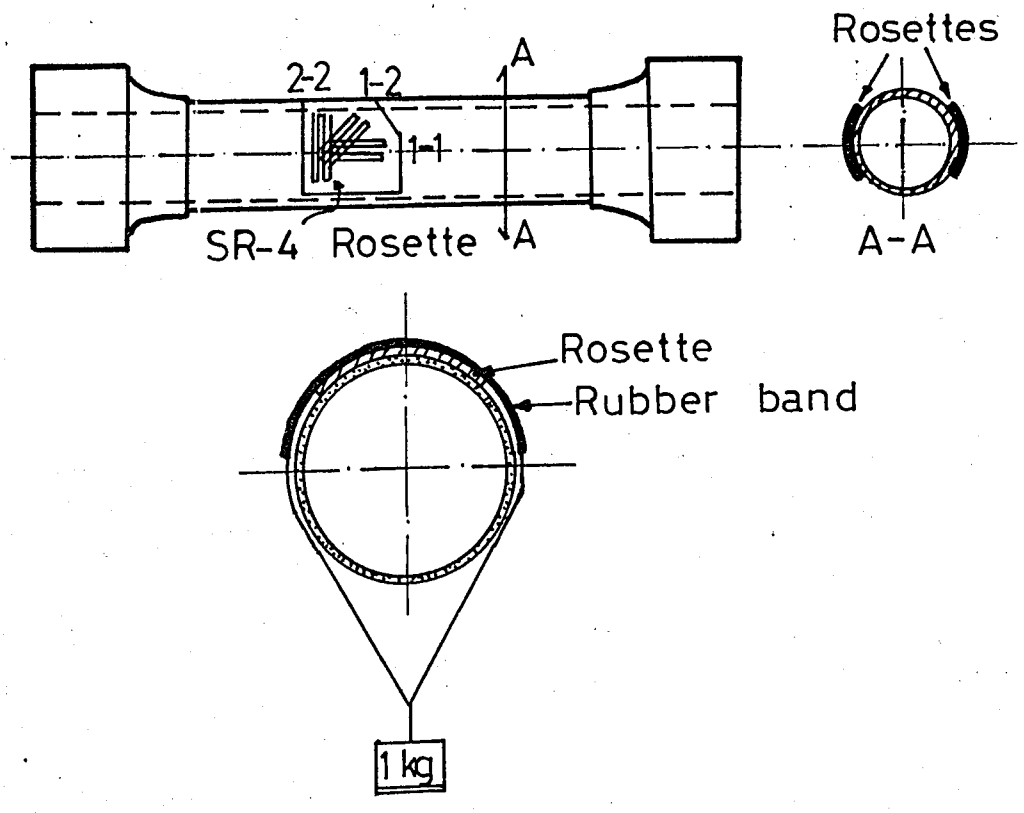

Figure 21. Sticking of rosettes to the specimen.

A dummy gage was also used to cancel the temperature effects. The gages have a gage factor of 2.04 and resistance of 120 ohms. In figure 22, connection of one gage to the strain indicator is shown.

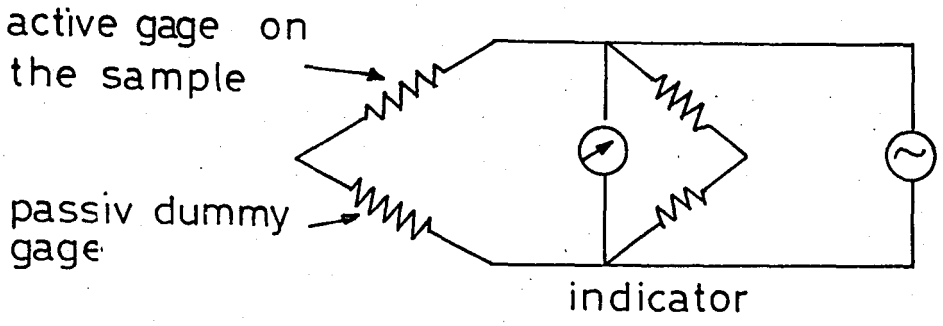

Figure 22. Connection diagram of one gage.

The specimen on which dummy gage was sticked was made up of the same material with our sample. The connections between the gages, channel sellector and the indicator is shown in figure 23.

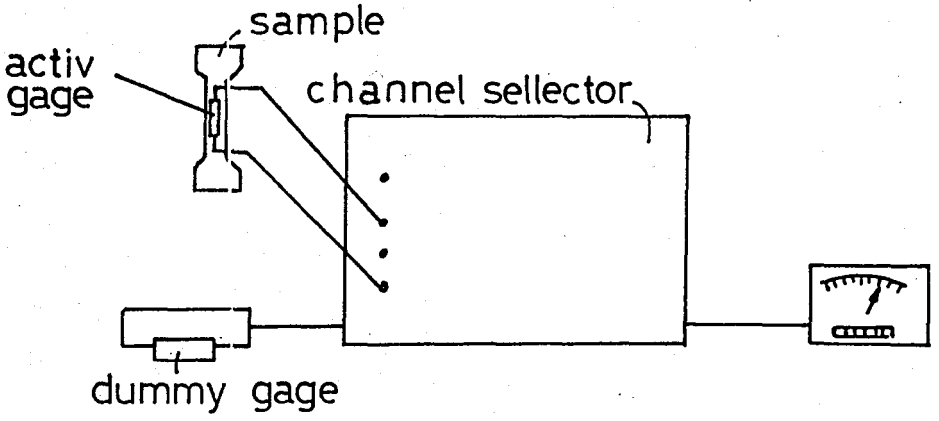

Figure 23. Connections between gages, channel sellector and indicator.

For correct reading the dummy gage and the active gages must have the same gage factors.

Before taking any reading, the gage factor dial must set to 2.04 ± % 1. Strain in the gage in microinches per inch was determined from the difference between setting of dial and switches before and after applying of stresses. Strains were read at the order of 10^{-6}. Strains are tension when positive and compression when negative.

Strains measured from each rosette were axial tensile strain ε_A, circumferencial ε_C, and 45 degree strain ε_{45}. Strains were recorded individually from each gage of each rosette.

The incremental strain in all three gages of a rosette increased appreciably in a short time following yielding. In all experiments strains were recorded as soon as possible after the increment was applied.

The strains of primary importance were the plastic shear strain γ_p and the plastic tensile strain ε_A. Increments in these strains due to increments in stress were computed from the plastic increments in ε_A, ε_C and ε_{45}.

In the experimental study, the normality condition was also tried to be found. The elastic deformation vector should be perpendicular to the yield curve of the yielding point. This is called the normality condition. At the yielding point tensile strain $\vec{\varepsilon}_1$ and shear strain $\vec{\varepsilon}_{12}$ were found and addition of these two vectors which is ε_{ij} was found. ε_{ij} should be perpendicular to the yield curve at that yield point (Fig.24).

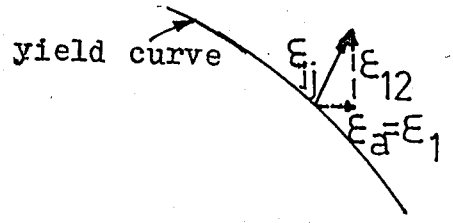

Figure 24. Normality condition.

ε_1 values were read directly from the indicator during the experiments. But ε_{12} values should be computed from the Mohr circle by using the readings of rosette values. The rosette used in these experiments can be shown schematically as in figure 25.

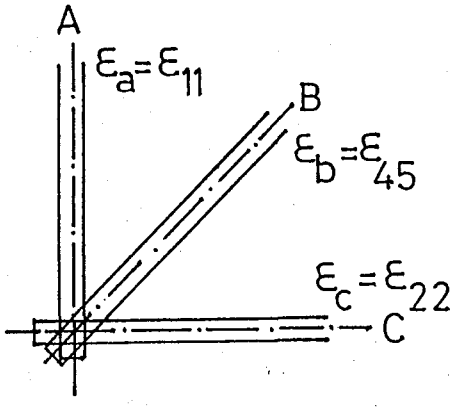

Figure 25. Schematic illustration of a rosette.

The Mohr circle in such a rosette can be drawn as shown in figure 26.

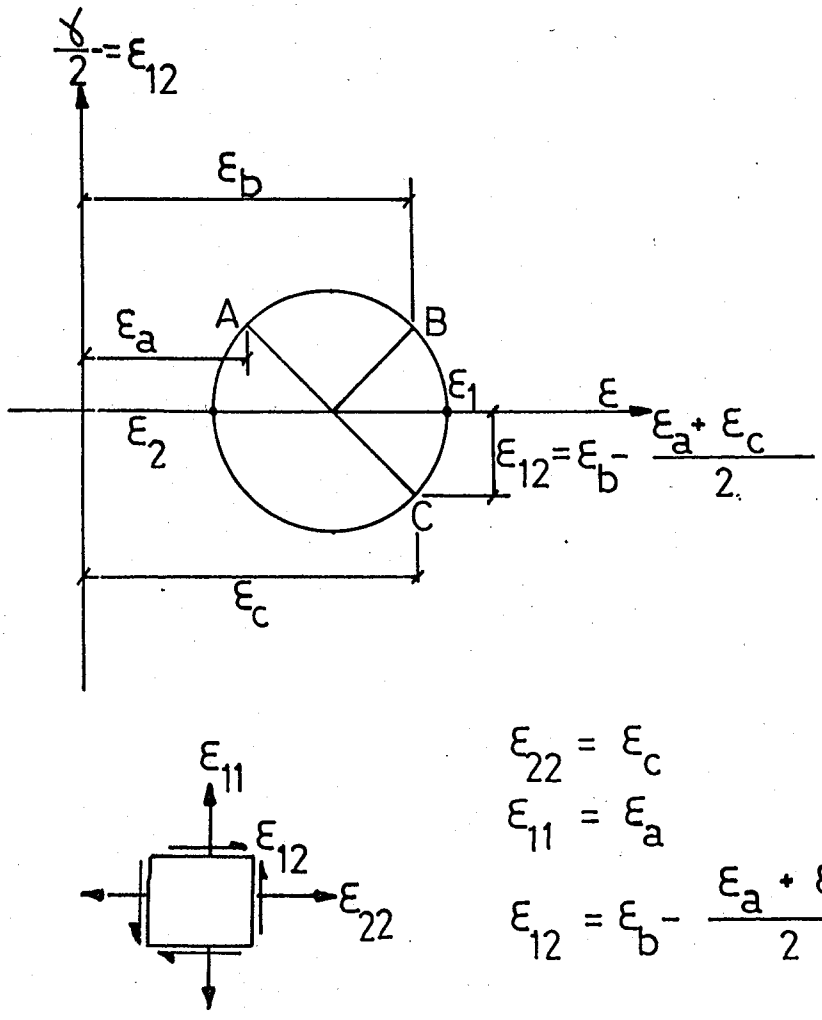

Figure 26. Mohr cirle.

$\Delta\varepsilon_{12}$ values were computed from the values of $\Delta\varepsilon$ read from the rosette at the yielding point. These values were plotted as $\Delta\varepsilon_{11}$ in the direction of σ, $\Delta\varepsilon_{12}$ in the direction of τ. Then $\Delta\varepsilon_{ij}$ was found and the normality condition was controlled.

IV. RESULTS

4.1. Annealed Aluminum (AA 1100)

4.1.1. Initial Yield Curve

A random sequence of probing was performed to determine the initial yield curve. The loading program is shown in figure 27. For the other yield curves the loading program will not be plotted. Similar programs were followed for them.

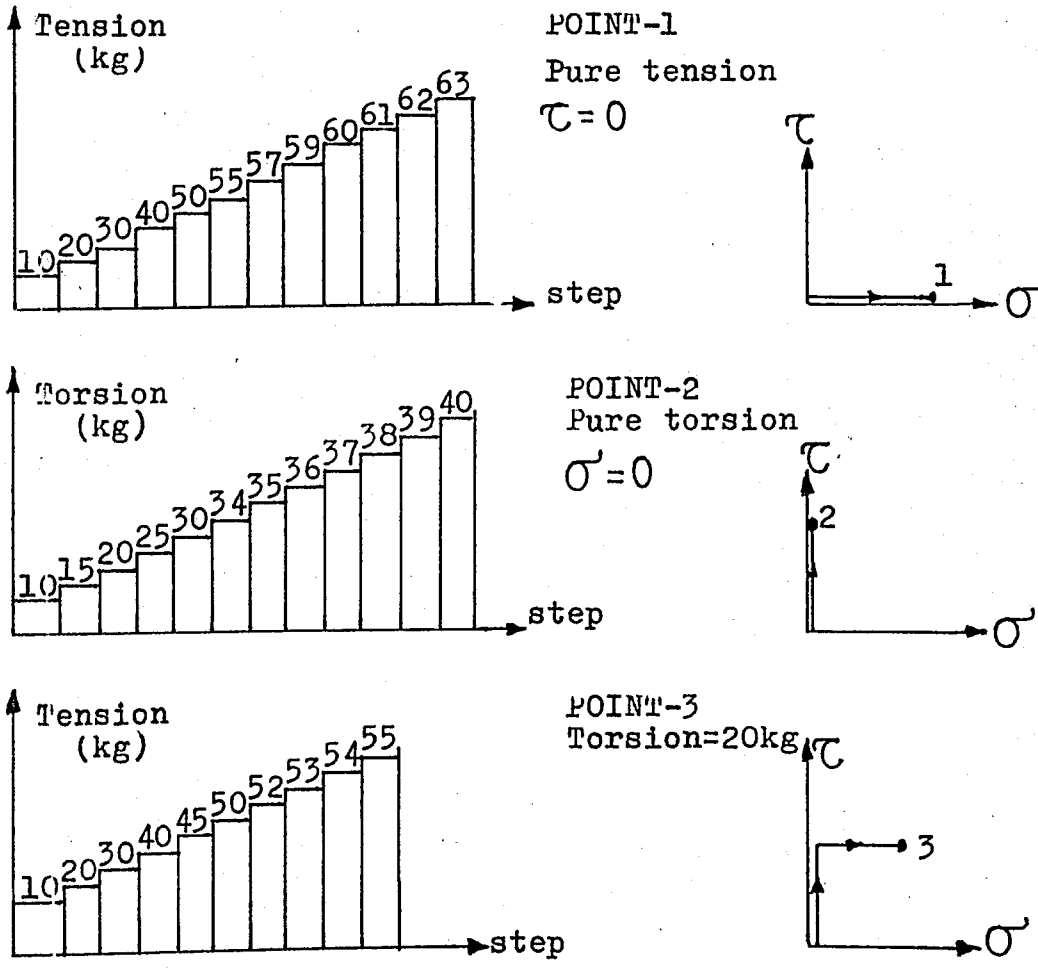

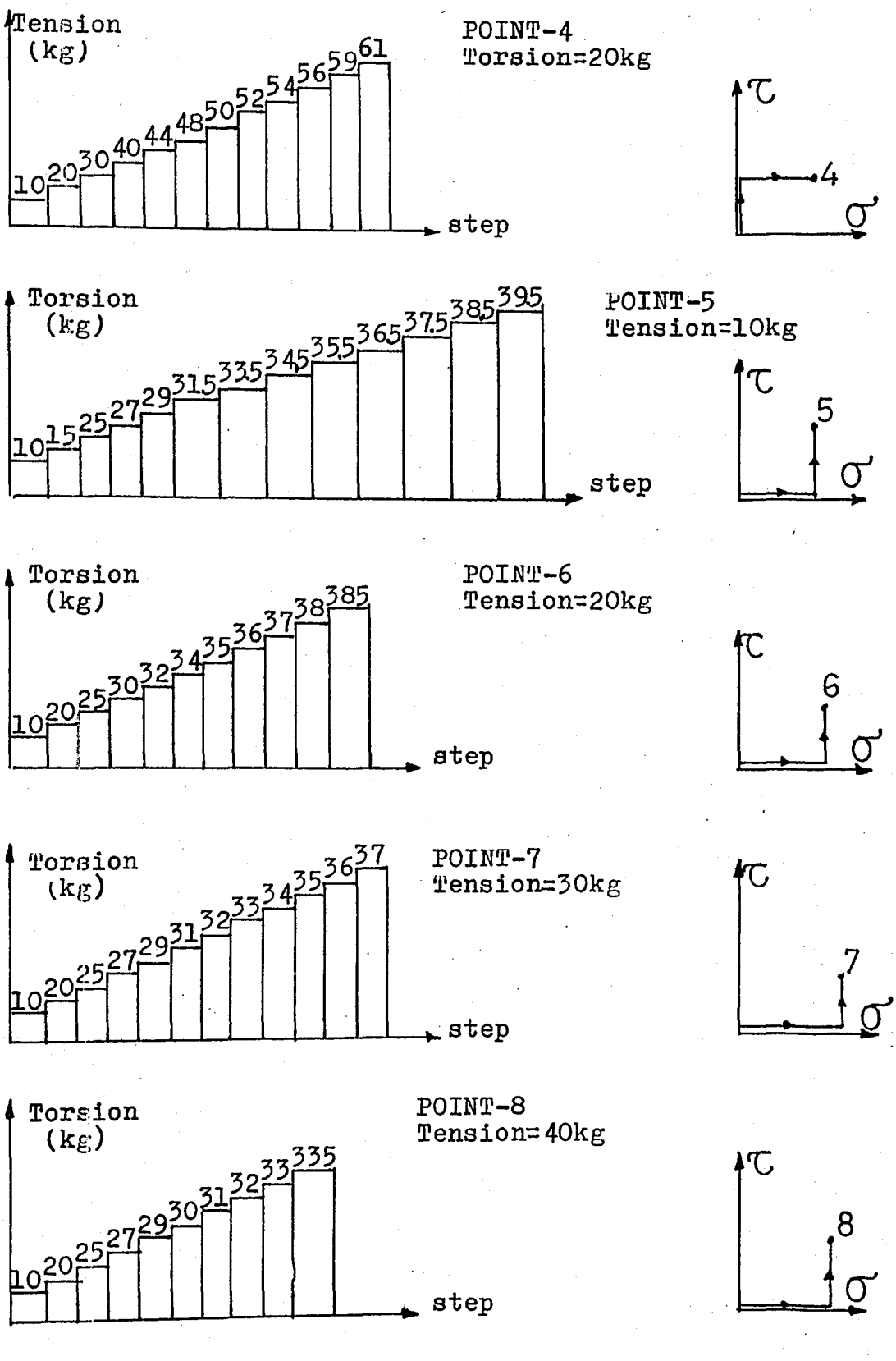
Tension
(kg)
10 20 30 40 44 48 50 52 54 56 59 61
step
POINT-4
Torsion=20kg
τ
4
σ
Torsion
(kg)
10 15 25 27 29 31.5 33.5 34.5 35.5 36.5 37.5 38.5 39.5
step
POINT-5
Tension=10kg
τ
5
σ
Torsion
(kg)
10 20 25 30 32 34 35 36 37 38 38.5
step
POINT-6
Tension=20kg
τ
6
σ
Torsion
(kg)
10 20 25 27 29 31 32 33 34 35 36 37
step
POINT-7
Tension=30kg
τ
7
σ
Torsion
(kg)
10 20 25 27 29 30 31 32 33 33.5
step
POINT-8
Tension=40kg
τ
8
σ

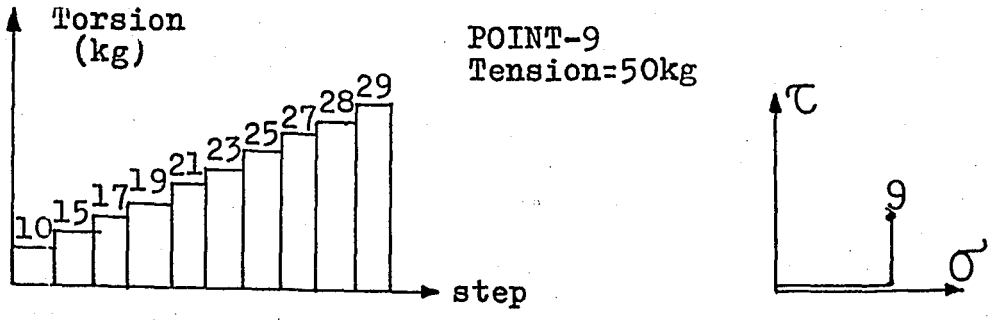

Fig.27 Loading program followed for the initial yield curve of annealed aluminum AA 1100 sample.

First the specimen was loaded in pure tension and in pure torsion. Next the specimen was loaded in shear probes. The permanent plastic strains were found for each point in order to control the normality condition. The stresses and the permanent plastic strains are tabulated in table 10.

Table 10. The stresses and the permanent plastic strains at the experimental points of the initial yield curve.

points	σ (kg/mm^2)	τ (kg/mm^2)	$\Delta\varepsilon_a$	$\Delta\varepsilon_{45}$	$\Delta\varepsilon_c$	$\Delta\varepsilon_{12}$
1	8.96	—	90	40	-40	15
2	—	5.15	-10	95	10	95
3	7.82	2.58	45	40	-40	37.5
4	8.68	1.29	50	10	-10	-10
5	1.42	5.02	25	40	-5	30
6	2.65	4.89	10	-85	-40	-70
7	4.27	4.70	60	-95	-30	-70
8	5.69	4.31	130	75	25	152
9	7.11	3.61	105	100	-15	65

The initial yield curve of the annealed aluminum is plotted in the figure 28.

Mises and Tresca ellipses are plotted in order to compare the initial yield curve with both criterion. The coordinates of the yield points on both Tresca and Mises ellipses were calculated and results are shown in table 11.

Table 11. Coordinates of some yield points.

$\sigma_y = 8.96$ kg/mm^2			
Mises Criteria		Tresca Criteria	
σ (kg/mm^2)	τ (kg/mm^2)	σ (kg/mm^2)	τ (kg/mm^2)
0	5.17	0	4.48
1	5.14	1	4.45
2	5.04	2	4.37
3	4.87	3	4.22
4	4.63	4	4.01
5	4.29	5	3.72
6	3.84	6	3.33
6.5	3.56	6.5	3.08
7	3.23	7	2.80
7.5	2.83	7.5	2.45
8	2.33	8	2.02
8.5	1.64	8.5	1.42

Von Mises and Tresca ellipses are shown in figure 28.

4.1.2. First Subsequent Yield Curve

After the obtaining of the initial yield curve, the sample was strain hardened under pure tension up to 10.8 kg/mm^2. By this way the sample was plastically deformed. The stresses and ΔE values for the points of the first subsequent yield curve are tabulated in table 12.

Table 12. The stresses and the permanent plastic strains at the experimental points of the first subsequent yield curve.

Points	σ (kg/mm^2)	τ (kg/mm^2)	ΔE_a	ΔE_{45}	ΔE_c	ΔE_{12}
1	10.24	——	120	20	-80	0
2	——	5.41	-40	100	-5	122.5
3	8.68	2.58	140	50	-40	0
4	7.4	3.86	105	130	-40	97.5
5	9.74	1.29	100	50	-30	15
6	1.42	5.67	-5	80	-5	85
7	2.85	5.41	40	115	-65	127.5
8	4.27	5.28	85	155	-20	122.5
9	4.99	5.22	40	-110	-50	-105
10	5.69	5.15	80	120	-40	100
11	6.4	4.89	90	100	-20	65
12	7.11	4.51	90	70	-40	45

First subsequent yield curve is shown in figure 29.

4.1.3. Second Subsequent Yield Curve

For further strain hardening, the sample was again plastically deformed. For this case it was strain hardened under pure torsion instead of pure tension up to 6.03 kg/mm^2. The stresses and $\Delta\varepsilon$ values for the points of the second subsequent yield curve are tabulated in table 13.

Table 13. The stresses and the permanent plastic strains at the experimental points of the second subsequent yield curve.

Points	σ (kg/mm^2)	τ (kg/mm^2)	$\Delta\varepsilon_a$	$\Delta\varepsilon_{45}$	$\Delta\varepsilon_c$	$\Delta\varepsilon_{12}$
1	——	6.18	-10	100	-10	110
2	8.61	——	95	-35	-50	-57.5
3	9.39	1.29	80	15	-20	15
4	9.32	1.93	60	35	-20	15
5	9.11	2.58	70	50	-15	22.5
6	8.11	3.86	60	70	-50	65
7	7.33	4.51	5	80	-40	75
8	1.42	5.92	20	105	5	97.5
9	2.85	5.86	10	35	-10	35
10	4.27	5.86	80	100	5	62.5
11	5.69	5.54	40	55	-20	45
12	6.40	5.34	140	160	-50	115
13	7.11	5.02	85	80	-20	47.5

The second subsequent yield curve is shown in Fig.30.

4.1.4. Third Subsequent Yield Curve

When the second subsequent yield curve was obtained, the sample was strain hardened once more in pure tension up to 10.95 kg/mm^2 and the third subsequent yield curve was obtained. The stresses and the $\Delta\varepsilon$ values for the points of this curve are tabulated in table 14.

Table 14. The stresses and the permanent plastic strains at the experimental points of the third subsequent yield curve.

Points	σ (kg/mm^2)	τ (kg/mm^2)	$\Delta\varepsilon_a$	$\Delta\varepsilon_{45}$	$\Delta\varepsilon_c$	$\Delta\varepsilon_{12}$
1	10.95	——	40	10	-15	-2.5
2	——	5.28	-20	80	15	82.5
3	10.39	1.29	20	70	-20	70
4	9.60	2.58	60	40	-45	32.5
5	8.39	3.86	55	90	10	67.5
6	1.42	5.54	0	25	-5	27.5
7	2.85	5.73	-5	50	-20	62.5
8	4.27	5.73	20	65	-15	62.5
9	5.69	5.54	30	55	-20	50
10	8.2	3.71	50	40	0	15

The third subsequent yield curve is shown in Fig.31.

4.1.5. Fourth Subsequent Yield Curve

After obtaining the third subsequent yield curve, the sample was plastically deformed in a different way. For this case it was strain hardened under proportional loading up to $\tau = 6.38$ kg/mm^2 and $\sigma = 3.52$ kg/mm^2. The stresses and $\Delta\varepsilon$ values for the points of the fourth subsequent yield curve are tabulated in table 15.

Table 15. The stresses and the permanent plastic strains at the experimental points of the fourth subsequent yield curve.

Points	σ (kg/mm^2)	τ (kg/mm^2)	$\Delta\varepsilon_a$	$\Delta\varepsilon_{45}$	$\Delta\varepsilon_c$	$\Delta\varepsilon_{12}$
1	9.96	——	105	-40	-50	-67.5
2	2.85	6.44	40	110	-40	110
3	——	6.31	-45	130	10	147.5
4	1.42	6.44	30	70	10	50
5	10.1	2.58	60	25	-40	15
6	5.69	5.67	30	70	-40	75
7	10.24	1.29	60	20	-30	5
8	9.11	3.86	70	90	-30	70
9	4.27	6.05	30	170	-25	167.5
10	7.68	5.15	40	45	-40	45

The fourth subsequent yield curve was shown in Fig.32. And for comparison all of the yield curves obtained experimentally is shown in figure 33.

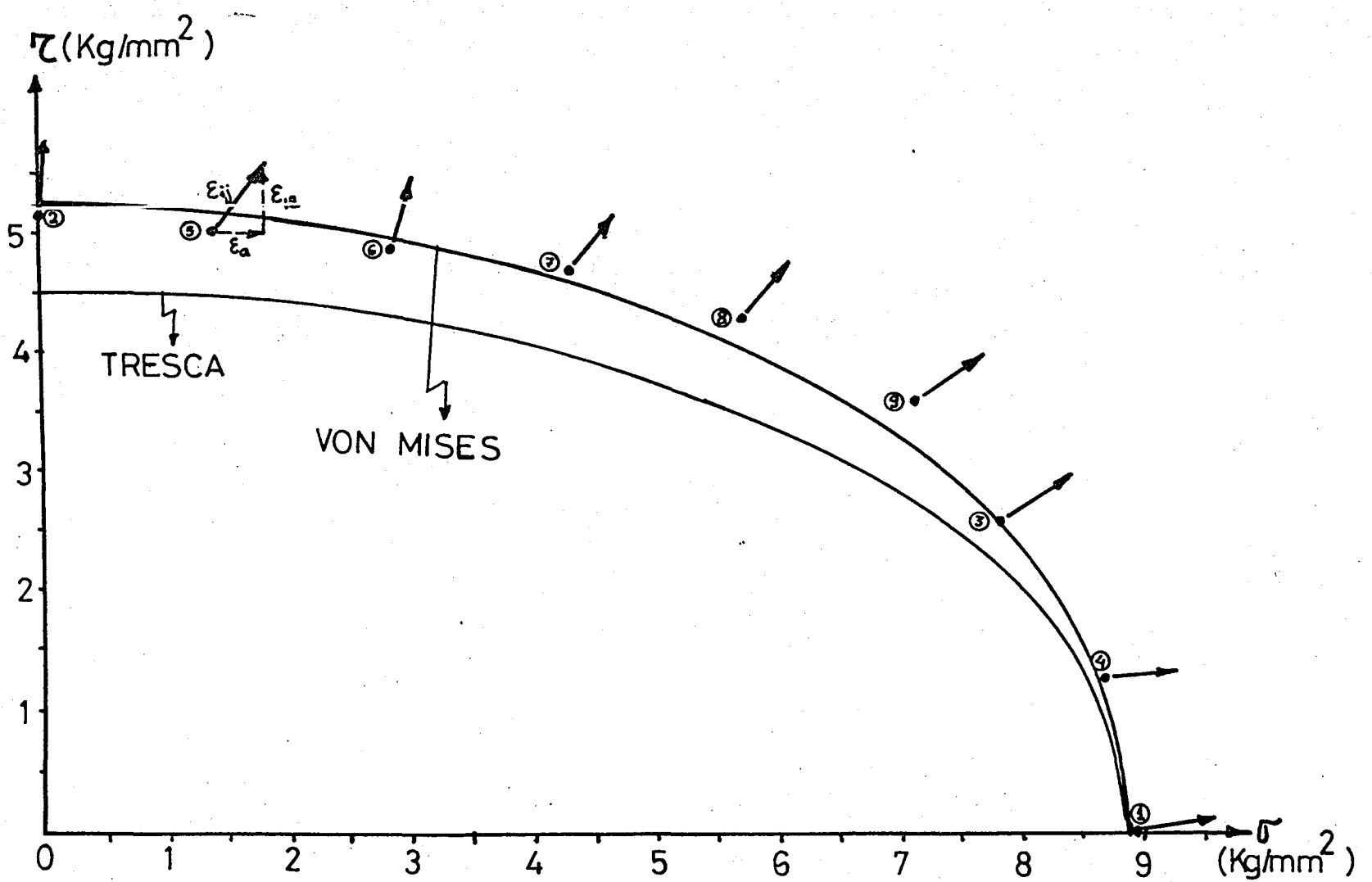

Figure 28. Von Mises and Tresca ellipses and experimental points of initial yield curve of annealed aluminum AA_1100.

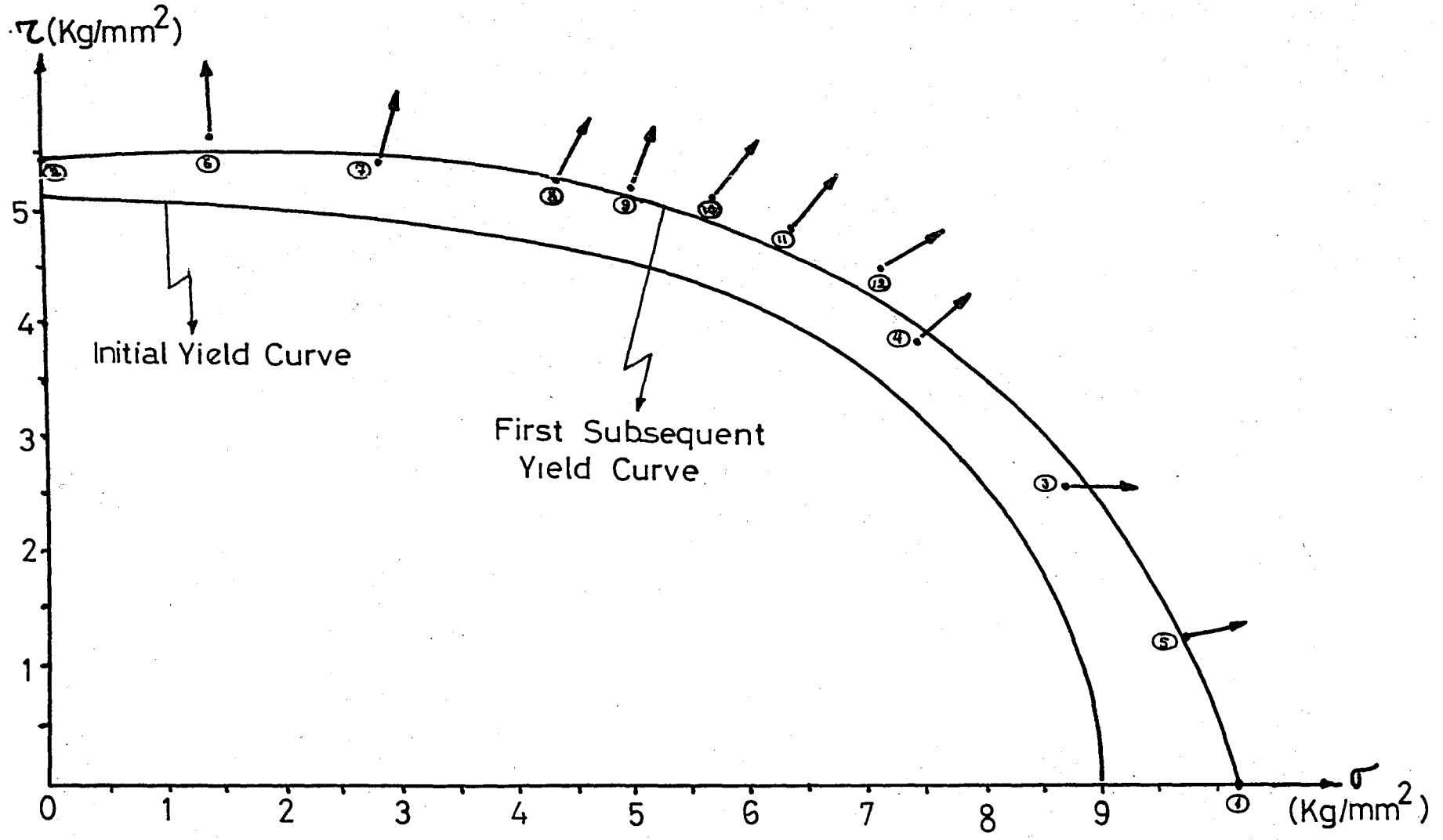

Figure 29. Initial and first subsequent yield curves of annealed aluminum AA_1100.

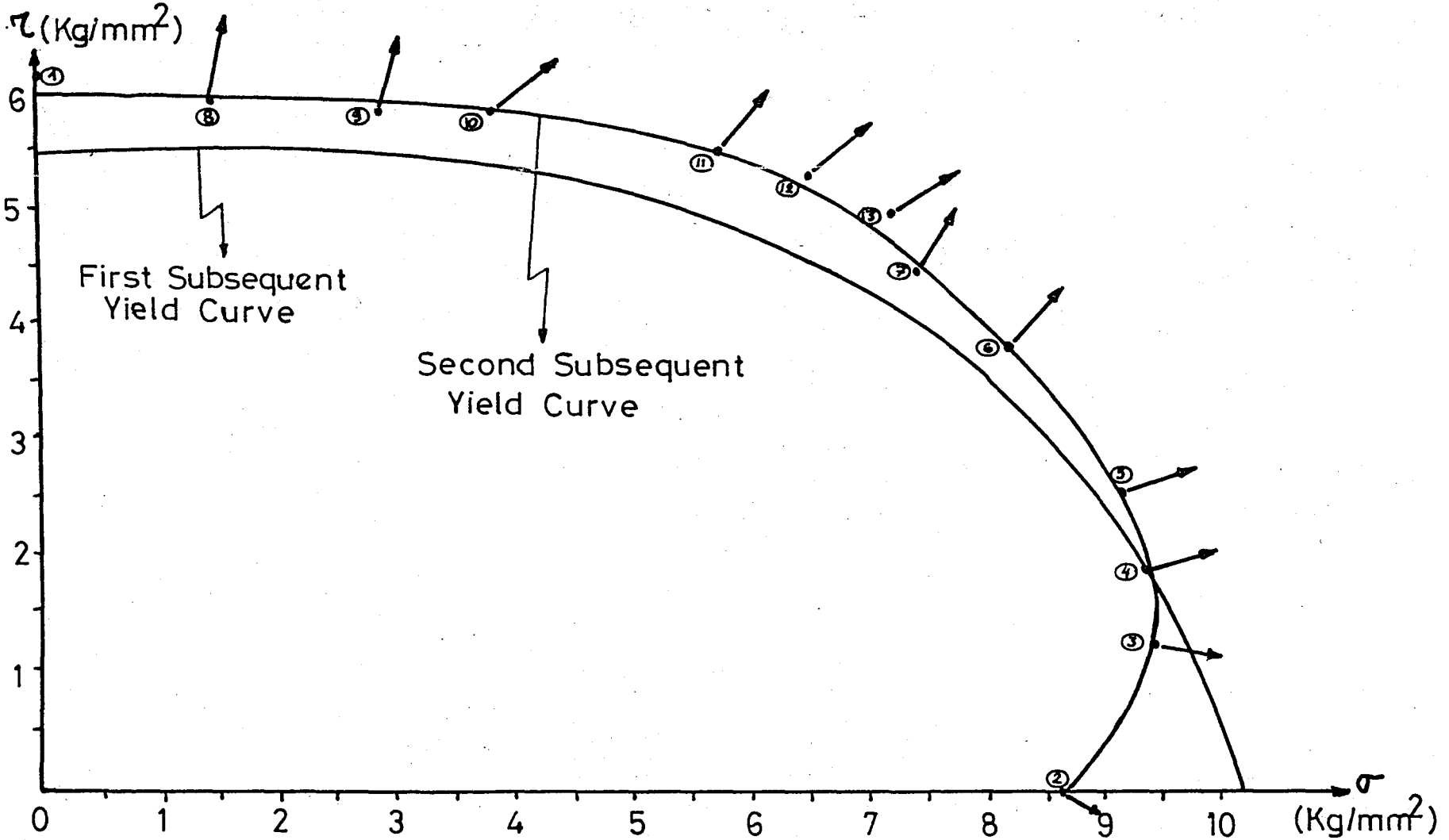

Figure 30. First and second subsequent yield curves of annealed aluminum AA_1100.

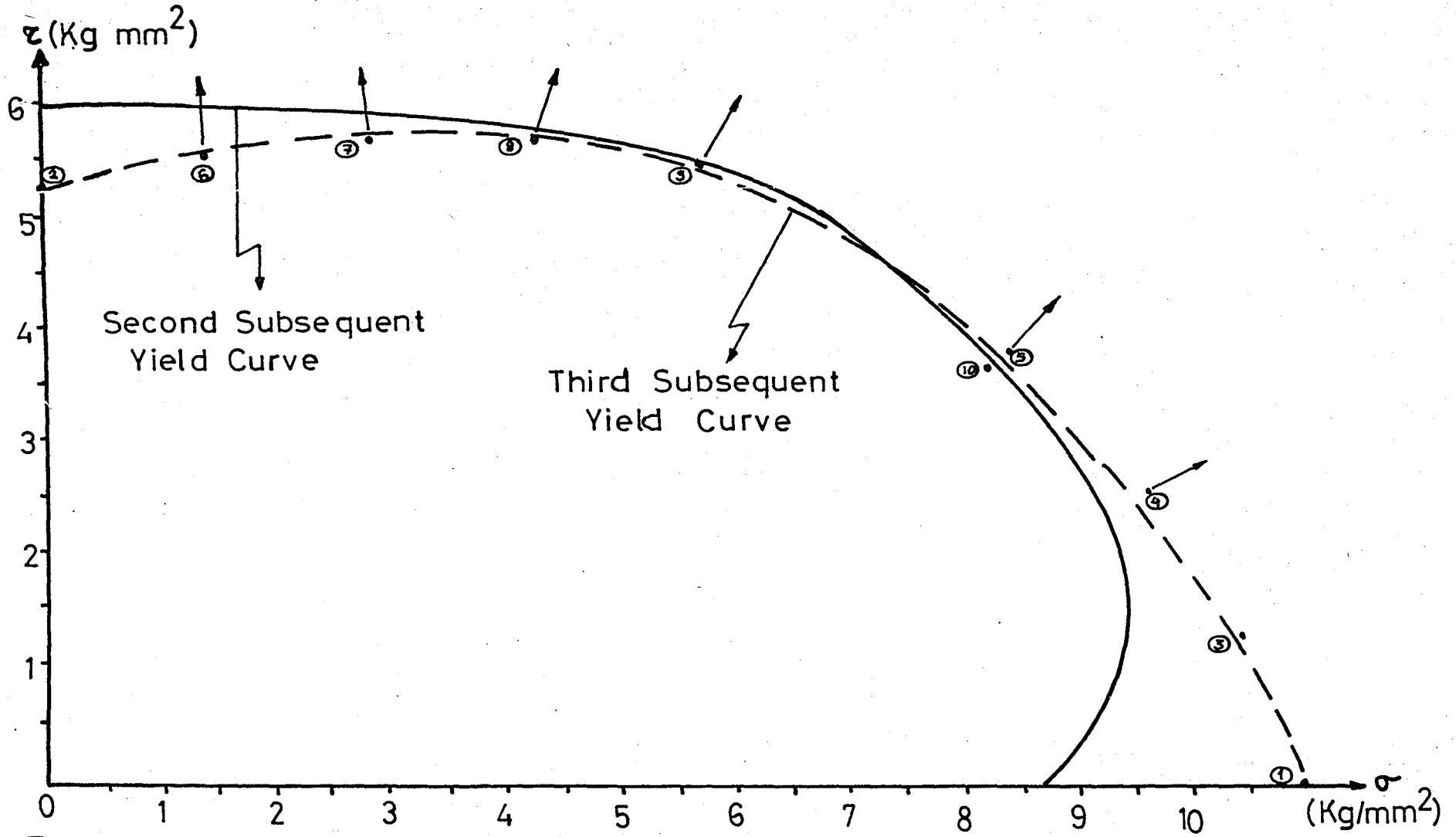

Figure 31. Second and third subsequent yield curves of annealed aluminum AA_1100.

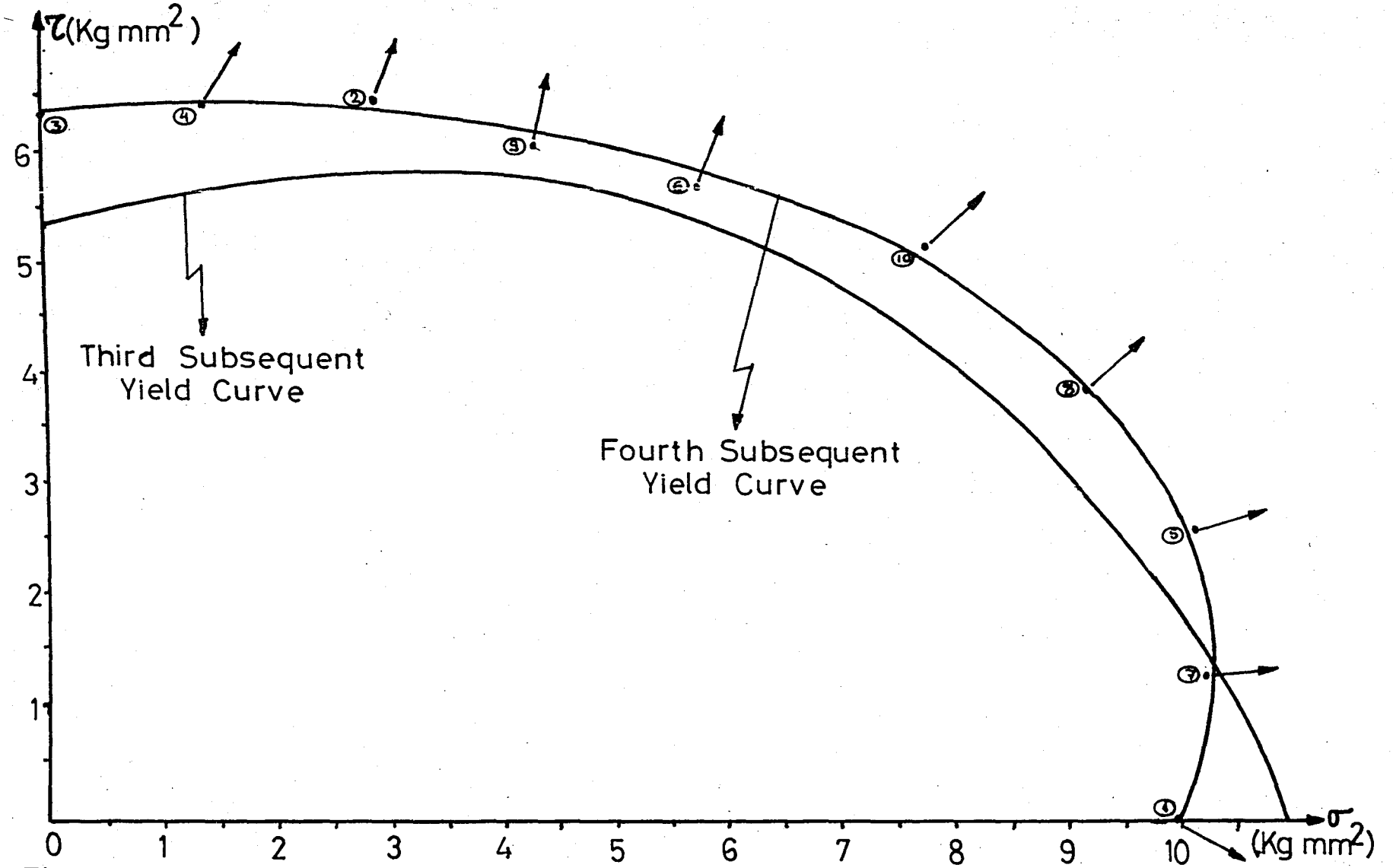

Figure 32. Third and fourth subsequent yield curves of annealed aluminum AA_1100.

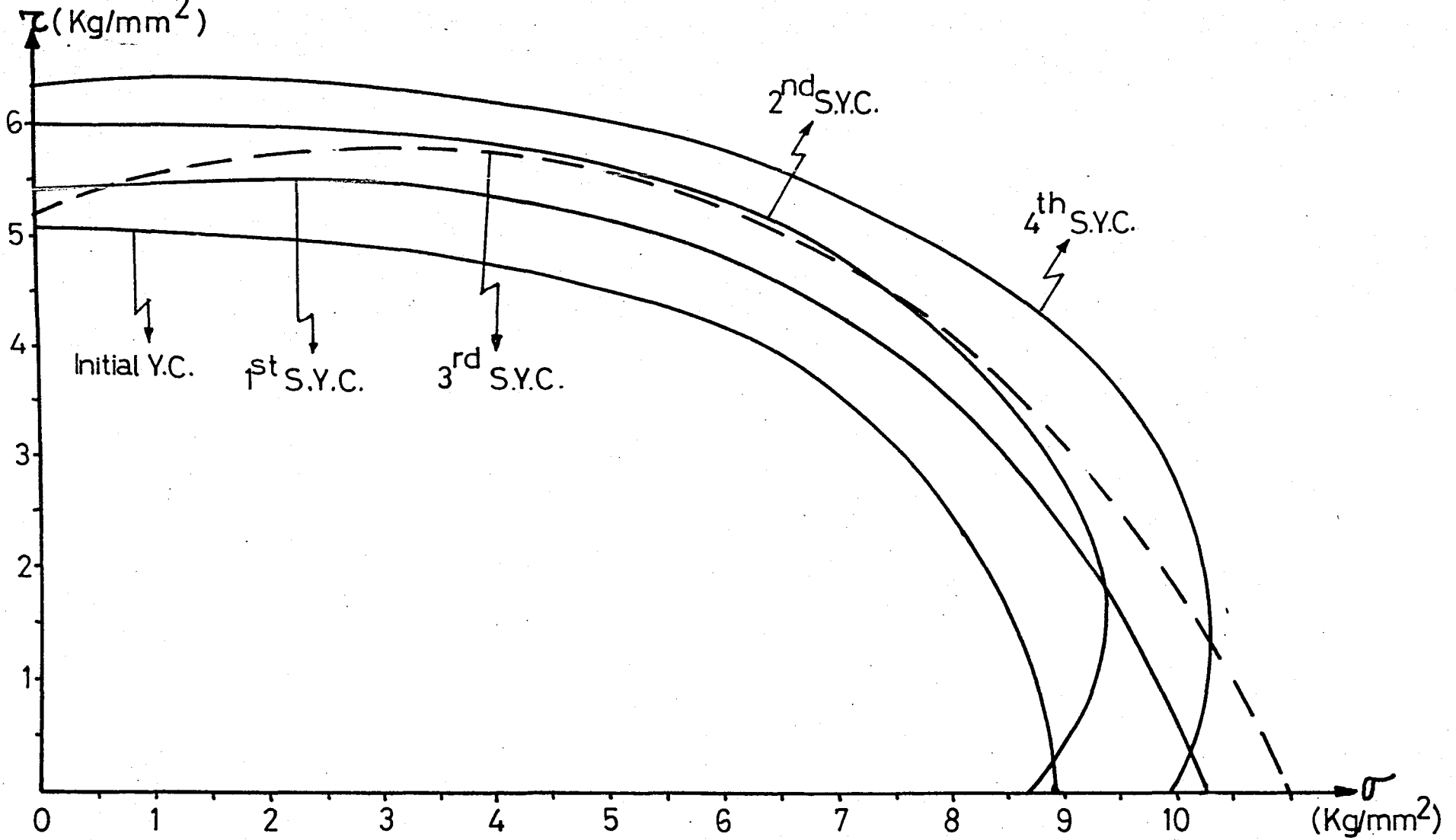

Figure 33. Yield curves obtained experimentally for annealed aluminum AA_1100.

4.2. Cast Aluminum

The second sample was cast aluminum. In order to obtain the initial yield curve, the sample was first loaded in tension. When the tensile stress was reached to 3.62 kg/mm^2, the sample suddenly fractured. At the time of fracture there was no plastic strain on the material. The material was in elastic range. The stress-strain curve is shown in Fig.34.

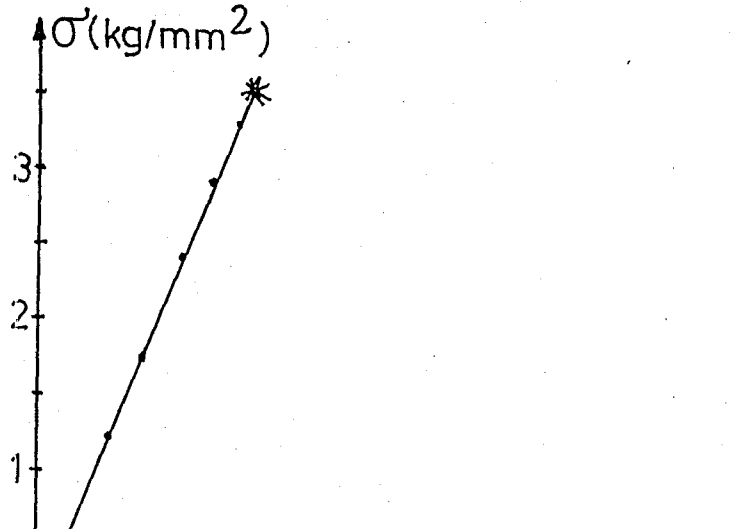

Figure 34. σ-ε curve of the cast aluminum sample.

From the σ-ε curve it is seen that fracture has occured within the elastic range without any plastic deformation. From here we can say that cast aluminums can not be tested on this combined tension-torsion machine. Because, this machine requires rather high plastic deformability from the materials.

4.3. Extruded Etial-60

4.3.1. Initial Yield Curve

A random sequence of probing was performed to determine the initial yield curve. First the sample was loaded in pure tension and in pure torsion. Next the specimen was loaded in shear probes and in proportional loading. The stresses and the strain increments at the experimental points of the initial yield curve are shown in table 16..

Table 16. The stresses and the permanent plastic strains ~~at~~ experimental points of the initial yield curve.

Points	σ (kg/mm^2)	τ (kg/mm^2)	$\Delta\varepsilon_a$	$\Delta\varepsilon_{45}$	$\Delta\varepsilon_c$	$\Delta\varepsilon_{12}$
1	4.9	——	90	25	-40	0
2	——	2.76	15	60	5	55
3	1.63	2.76	25	50	-20	47.5
4	4.74	0.75	130	55	-55	17.5
5	2.62	2.69	40	55	-25	47.5
6	3.27	2.54	35	30	-35	30
7	4.58	1.49	55	45	-20	27.5
8	4.25	2.10	40	25	-40	25

The initial yield curve of the extruded ETIAL-60 is plotted in figure 35.

Mises and Tresca ellipses are also ploted in order to compare the initial yield curve with both criteria. The coordinates of the initial yield points on both Tresca and Mises ellipses are shown in table 17.

Table 17. Coordinates of some yield points.

$\sigma_y = 4.90$ kg/mm^2			
Mises Criteria		Tresca Criteria	
σ (kg/mm^2)	τ (kg/mm^2)	σ (kg/mm^2)	τ (kg/mm^2)
0	2.45	0	2.83
0.5	2.44	0.5	2.81
1	2.40	1	2.77
1.5	2.33	1.5	2.69
2	2.24	2	2.58
3	1.94	3	2.24
4	1.42	4	1.63
4.5	0.97	4.5	1.12
4.9	0	4.9	0

Von Mises and Tresca ellipses are shown in Fig.35.

4.3.2. First Subsequent Yield Curve

In order to see the strain hardening character of extruded ETİAL-60, the sample was plastically deformed first under pure tension up to 6.2 kg/mm^2. The stresses and $\Delta\varepsilon$ values for the points of the first subsequent yield curve are given in table 18.

Table 18. The stresses and $\Delta\varepsilon$ values for the points of the first subsequent yield curve.

Points	σ (kg/mm^2)	τ (kg/mm^2)	$\Delta\varepsilon_a$	$\Delta\varepsilon_{45}$	$\Delta\varepsilon_c$	$\Delta\varepsilon_{12}$
1	6.21	—	45	20	-20	7.5
2	—	3.13	-30	110	20	115
3	1.63	3.13	50	60	-10	40
4	3.27	2.84	70	70	-30	50
5	5.23	1.49	70	40	-30	20
6	4.58	2.24	60	50	-25	32.5
7	4.25	2.61	65	50	-15	25

The first subsequent yield curve is shown in figure 36.

4.3.3. Second Subsequent Yield Curve

After obtaining of the first subsequent yield curve, the sample was strain hardened under pure torsion up to 3.88 kg/mm^2. By this way the sample was plastically deformed. The stresses and $\Delta\varepsilon$ values for the points of the second subsequent yield curve are tabulated in table 19.

Table 19. The stresses and $\Delta\varepsilon$ values for the points of the second subsequent yield curve.

Points	σ (kg/mm^2)	τ (kg/mm^2)	$\Delta\varepsilon_a$	$\Delta\varepsilon_{45}$	$\Delta\varepsilon_c$	$\Delta\varepsilon_{12}$
1	5.72	——	150	0	-50	-50
2	——	3.88	0	90	20	80
3	5.80	0.75	25	-30	-60	-12.5
4	1.63	3.73	50	120	-5	97.5
5	5.64	1.49	75	50	-35	30
6	3.27	3.21	30	35	-20	30
7	5.23	2.24	60	35	-30	20
8	4.10	3.06	20	30	-30	35
9	4.90	2.76	80	60	-50	45
10	4.66	2.99	95	95	-15	55

The second subsequent yield curve is shown in Fig.37. And for comparison all of the yield curves obtained experimentally are shown in figure 38.

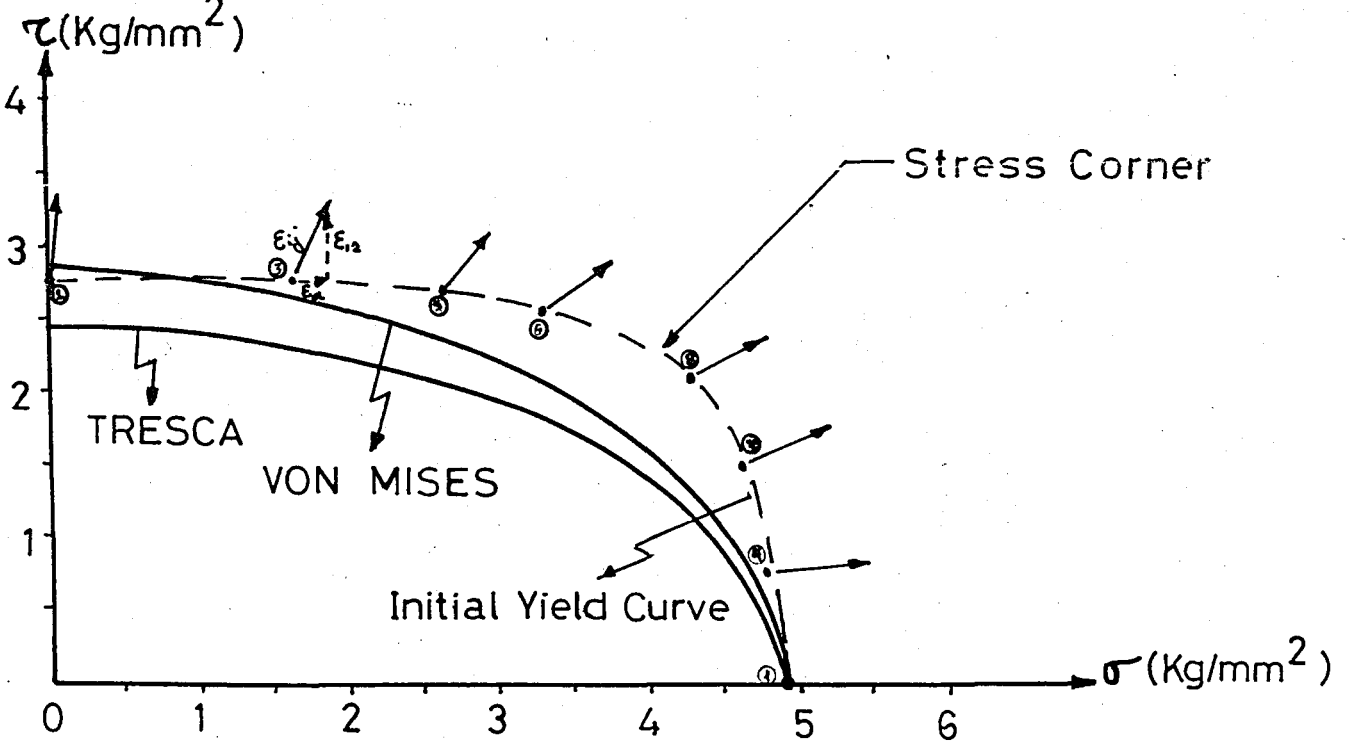

Figure 35. Tresca and von Mises ellipses and initial yield curve of extruded ETİAL-60.

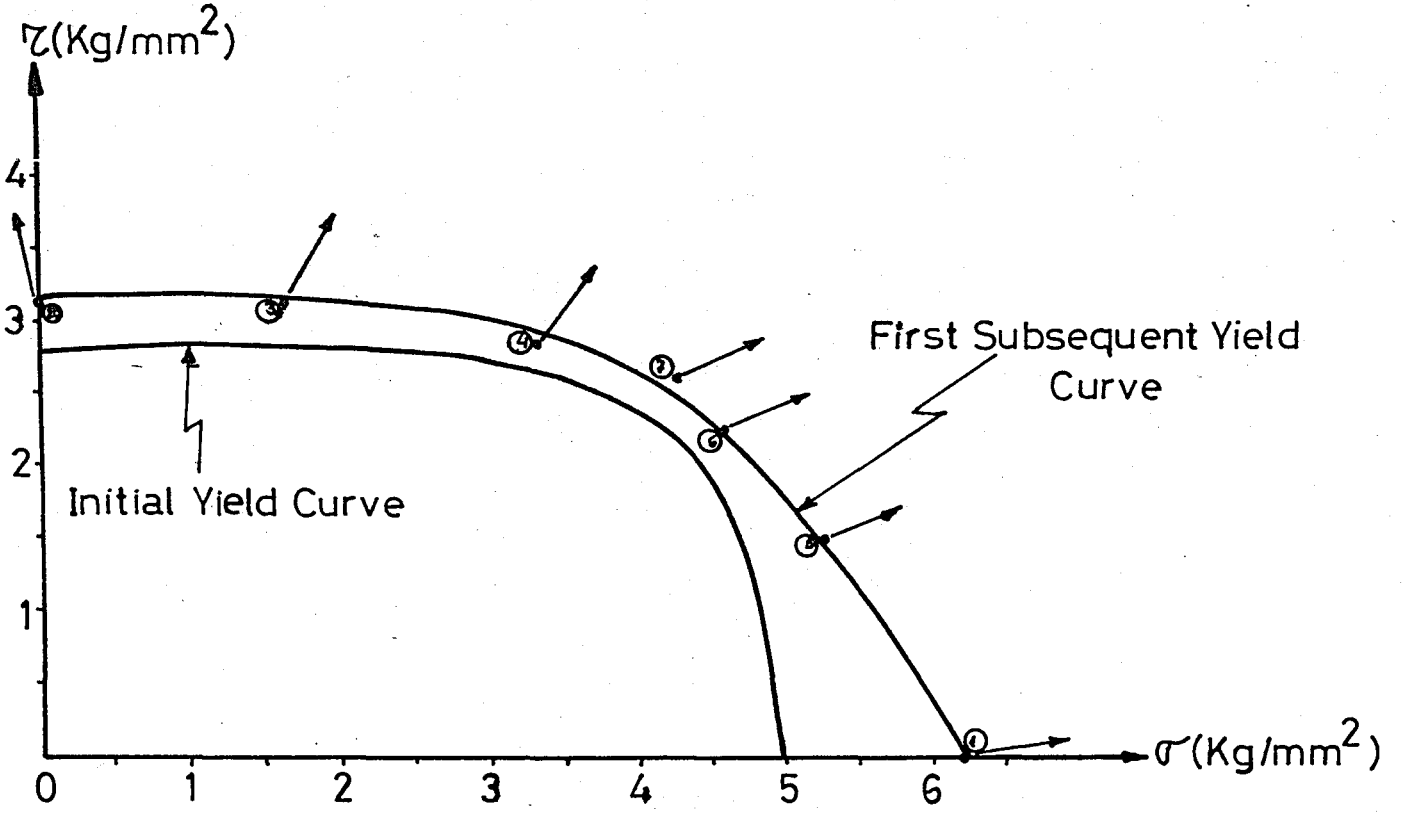

Figure 36. Initial and first subsequent yield curves of extruded ETİAL-60.

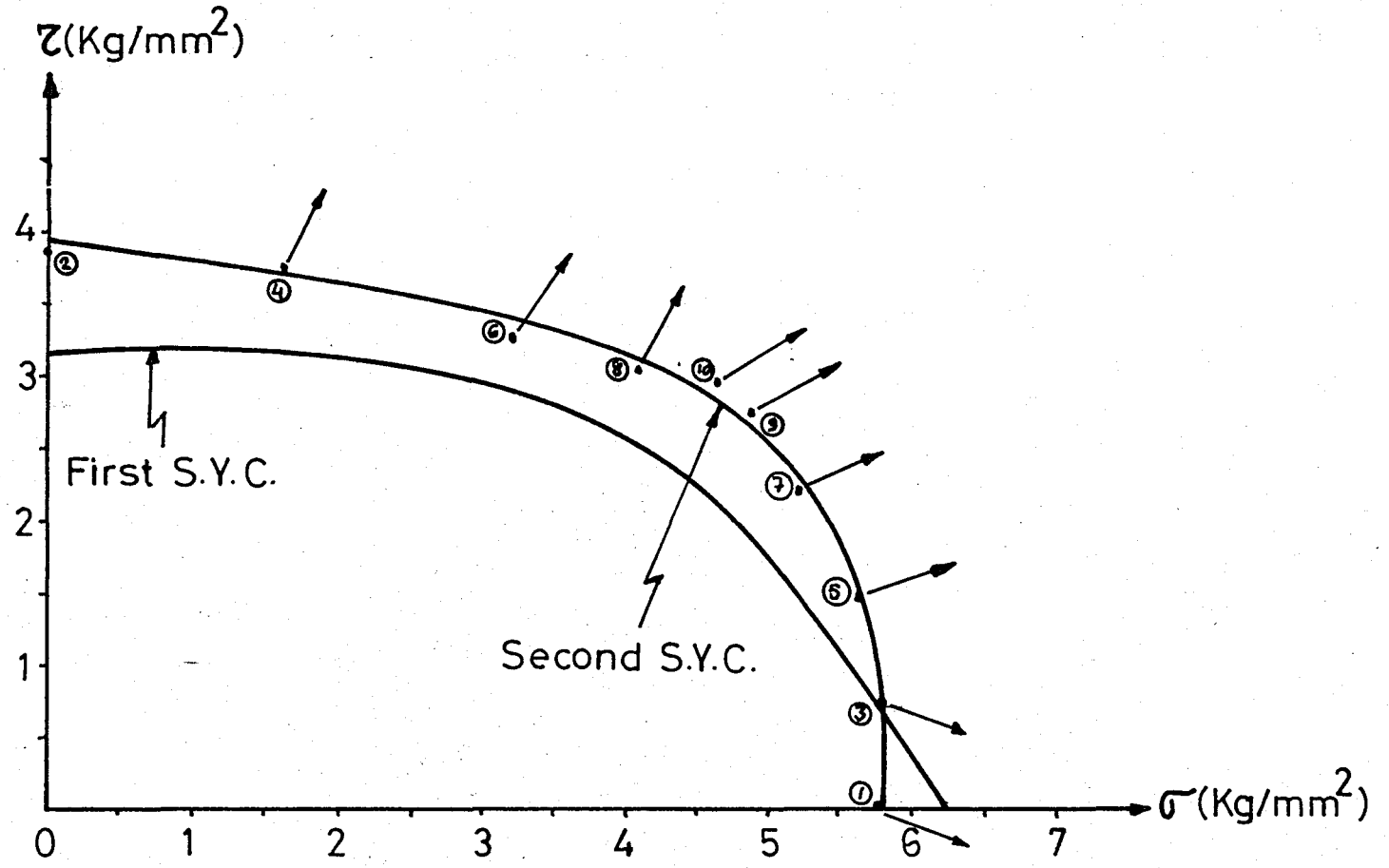

Figure 37. First and second subsequent yield curves of extruded ETİAL-60.

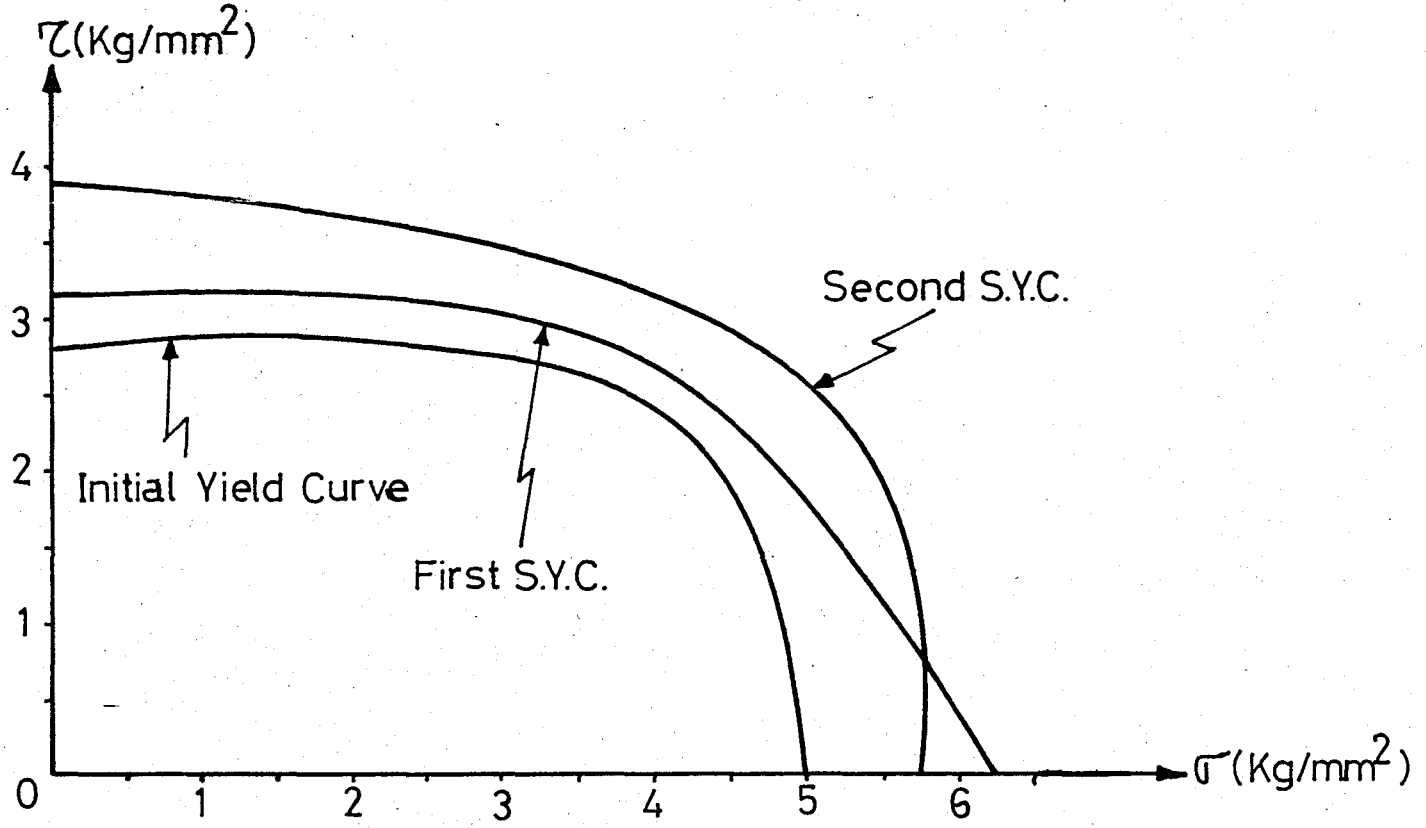

Figure 38. Initial and subsequent yield curves of extruded ETİAL-60.

4.4. Age-Hardened ETİAL-60

4.4.1. Initial Yield Curve

A random sequence of probing was performed to determine the initial yield curve. First the sample was loaded in pure tension and in pure torsion. Next the specimen was loaded in shear probes and in proportinal loadings. The stresses and ΔE values at the experimental points of the initial yield curve are shown in table 20.

Table 20. The stresses and ΔE values at the experimental points of the initial yield curve.

Points	σ (kg/mm^2)	τ (kg/mm^2)	ΔE_a	ΔE_{45}	ΔE_c	ΔE_{12}
1	10.40	——	65	30	-25	10
2	——	4.48	-55	185	10	207.5
3	9.81	1.49	120	50	-55	17.5
4	8.58	2.99	145	175	-45	125
5	1.64	4.55	5	95	5	90
6	3.27	4.63	10	70	-15	72.5
7	7.60	3.73	120	140	-50	105
8	6.21	4.48	120	285	-40	245
9	4.09	4.70	20	40	-10	35
10	4.90	4.78	20	90	-20	90

The initial yield curve of the age-hardened aluminum is shown in figure 39.

Mises and Tresca ellipses are again plotted in order to compare the initial yield curve with both criteria . The coordinates of the initial yield points on both Tresca and Mises ellipses are shown in table 21.

Table 21. Coordinates of some yield points.

$\sigma_y = 10.4$ kg/mm^2			
Mises Criteria		Tresca Criteria	
(kg/mm^2)	(kg/mm^2)	(kg/mm^2)	(kg/mm^2)
0	6	0	5.20
1	5.98	1	5.18
2	5.89	2	5.10
3	5.75	3	4.99
4	5.54	4	4.80
5	5.26	5	4.56
6	4.90	6	4.25
7	4.44	7	3.85
8	3.84	8	3.32
9	3.01	9	2.61
9.5	2.44	9.5	2.12
10	1.66	10	1.43

Von Mises and Tresca ellipses are shown in figure 39.

4.4.2. First Subsequent Yield Curve

When the initial yield curve was obtained, extruded ETİAL-60 sample was strain hardened by plastically deforming under pure tension up to 11.4 kg/mm^2. The stresses and permanent plastic strains for the points of the first subsequent yield curve are tabulated in table 22.

Table 22. The stresses and $\Delta\varepsilon$ values at the experimenta points of the first subsequent yield curve.

Points	σ (kg/mm^2)	τ (kg/mm^2)	$\Delta\varepsilon_a$	$\Delta\varepsilon_{45}$	$\Delta\varepsilon_c$	$\Delta\varepsilon_{12}$
1	11.36	——	110	20	-45	12.5
2	——	4.93	-80	220	20	250
3	1.63	4.93	20	65	5	52.5
4	10.55	1.49	240	65	-70	-20
5	3.27	4.93	5	135	-5	135
6	9.16	2.99	90	85	-45	62.5
7	4.90	4.85	30	110	-10	100
8	8.34	3.73	80	95	-50	80
9	7.19	4.33	50	55	-30	45

The first subsequent yield curve is shown in figure 40.

4.4.3. Second Subsequent Yield Curve

After obtaining of the first subsequent yield curve, the sample was then strain hardened under pure torsion up to τ=5.15 kg/mm^2.. By this way the sample was plastically deformed. The stresses and $\Delta\varepsilon$ values for the points of the second subsequent yield curve are tabulated in table 23.

Table 23. The stresses an $\Delta\varepsilon$ values at the points of the second subsequent yield curve.

Points	(kg/mm^2)	(kg/mm^2)	$\Delta\varepsilon_a$	$\Delta\varepsilon_{45}$	$\Delta\varepsilon_c$	$\Delta\varepsilon_{12}$
1	10.63	——	130	-50	-60	-85
2	——	5.15	-50	-50	20	-22.5
3	1.63	5.15	35	50	0	32.5
4	3.27	5.15	20	100	85	47.5
5	10.63	1.49	100	-30	-55	-52.5
6	9.65	2.99	100	95	0	45
7	7.36	4.48	110	205	-45	172.5
8	4.9	4.90	30	50	0	35

The second subsequent yield curve is shown in Fig.41. And for comparison all of the yield curves obtained experimentally are shown in figure 42.

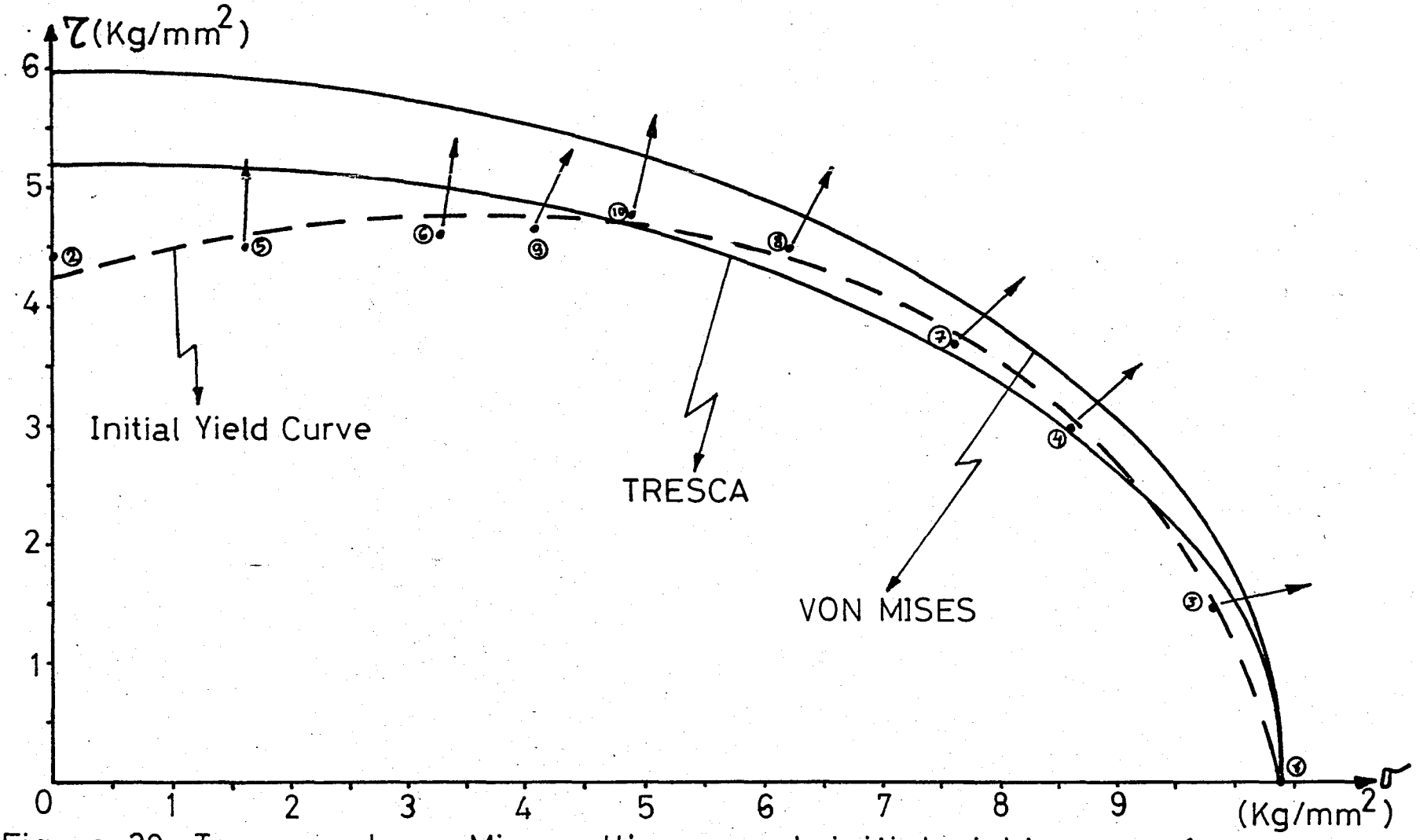

Figure 39. Tresca and von Mises ellipses and initial yield curve of age-hardened ETİAL-60.

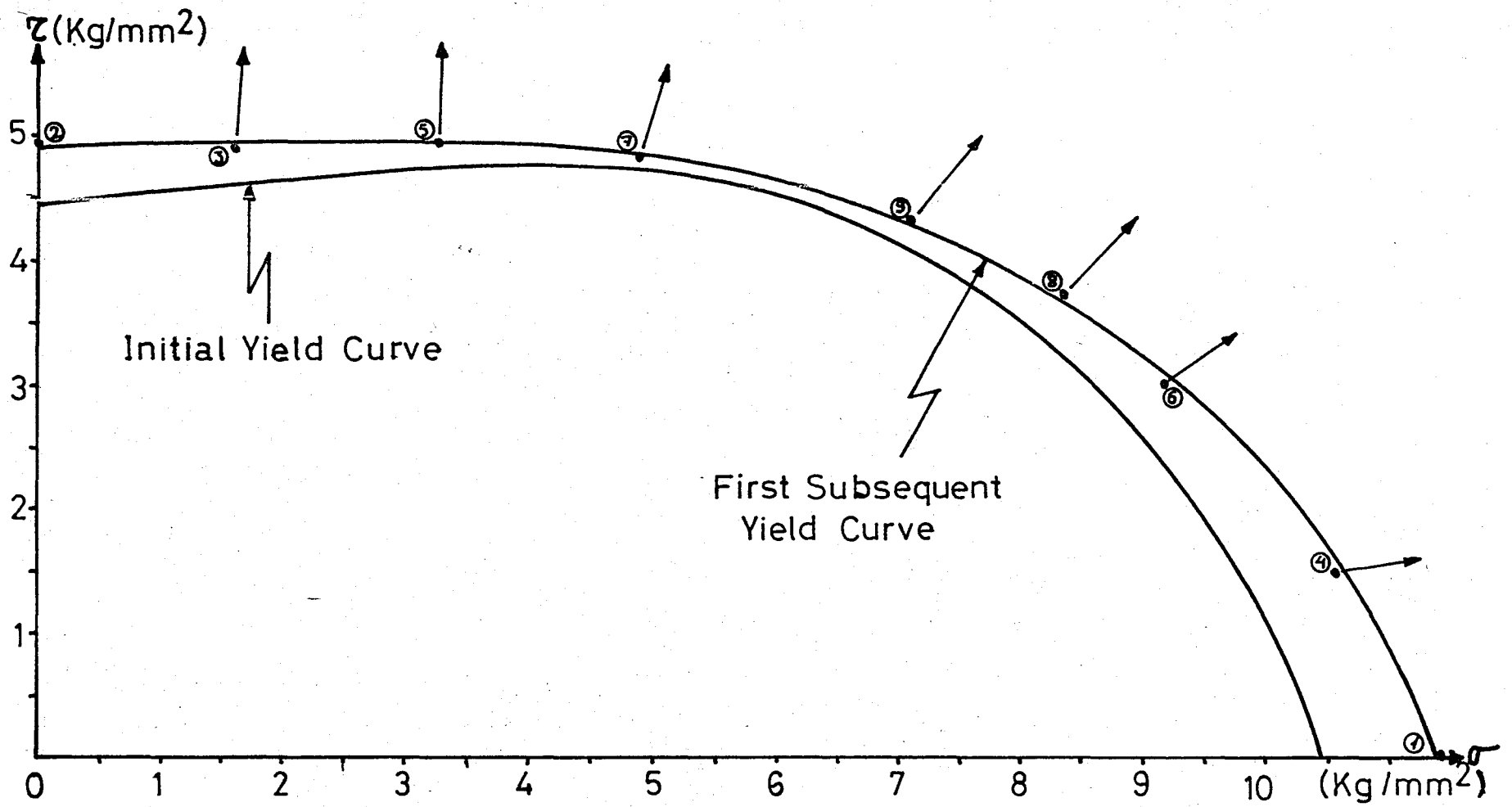

Figure 40. Initial and first subsequent yield curves of age-hardened aluminum ETİAL-60.

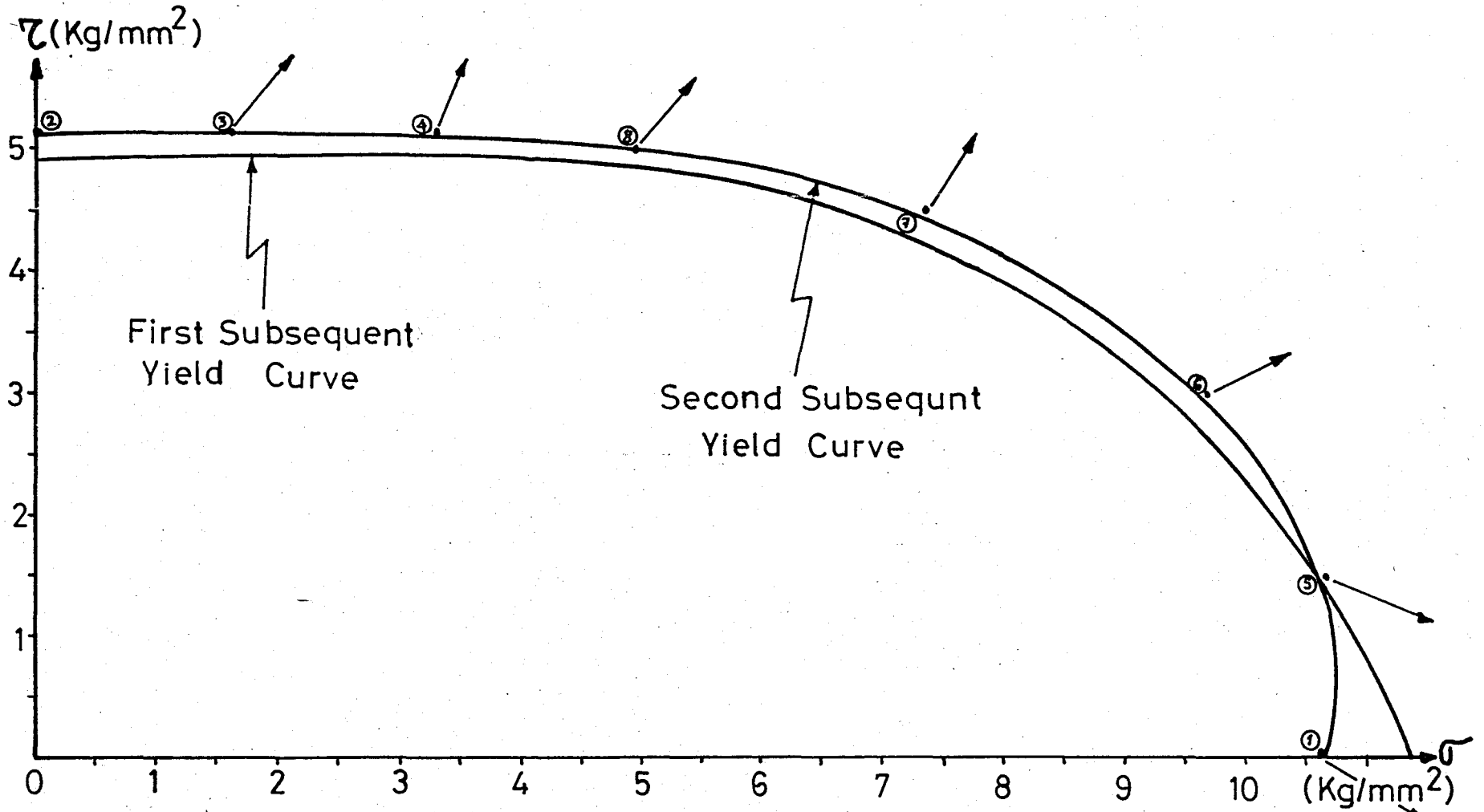

Figure 41. First and second subsequent yield curves of age-hardened aluminum ETİAL-60.

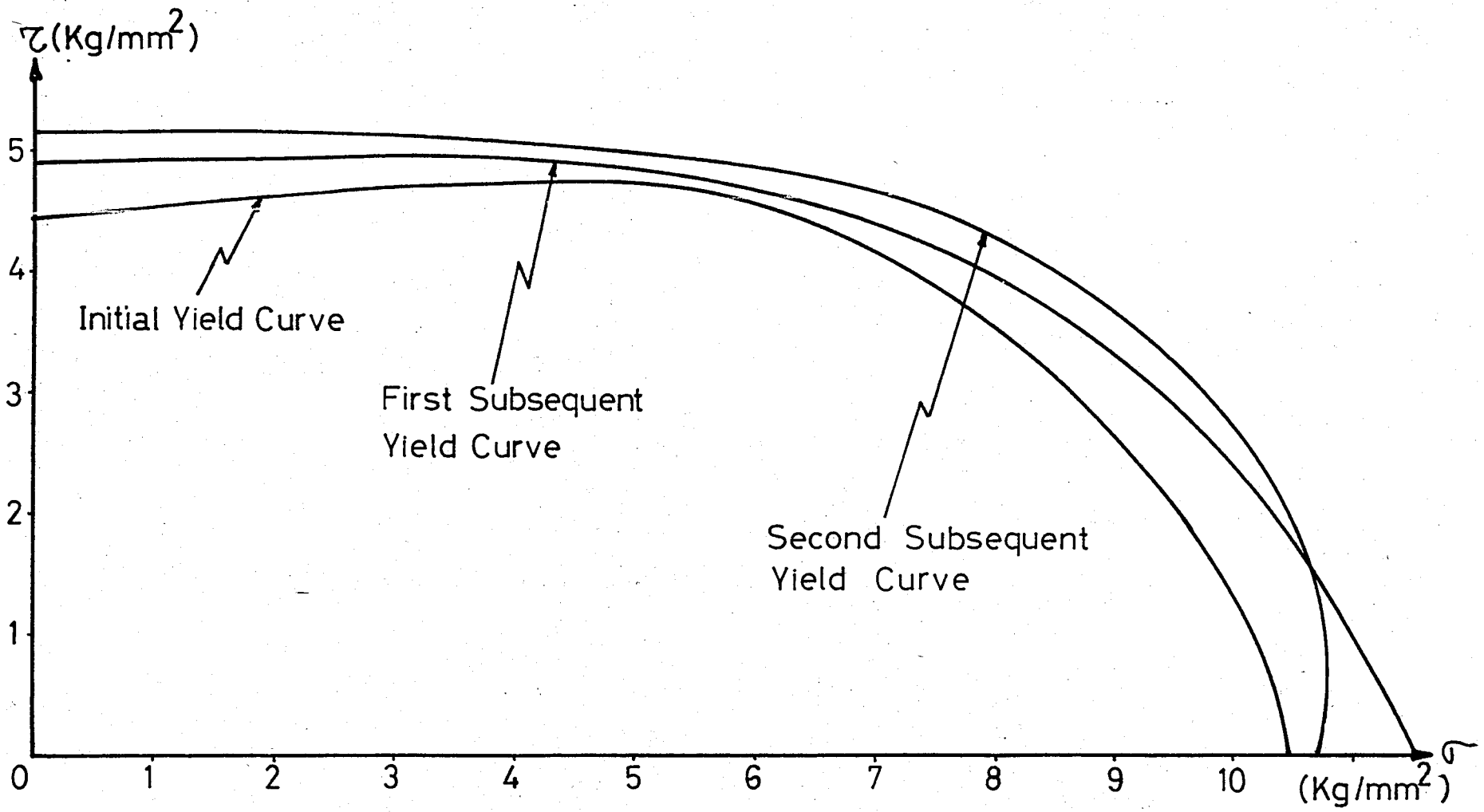

Figure 42. Initial and subsequent yield curves of age-hardened aluminum ETİAL-60.

4.5. Polyethylene

4.5.1. Initial Yield Curve

A random sequence of probing was performed to determine the initial yield curve. First the sample was loaded in pure tension and in pure torsion. Next the specimen was loaded in shear probes and in proportional loadings. The stresses at the experimenta points of the initial yield curve are shown in the table 24.

Table 24. The stresses at the experimental points of the initial yield curve.

Points	σ (kg/mm^2)	τ (kg/mm^2)
1	0.53	——
2	——	0.328
3	0.5	0.18
4	0.21	0.42
5	0.53	0.11
6	0.47	0.273
7	0.29	0.38

Mises and Tresca ellipses are also plotted in order to compare the initial yield curve with both criteria . The coordinates of the initial yield points on both Tresca and Mises ellipses are shown in table 25.

Table 25. Coordinates of some yield points.

$\sigma_y = 0.53$ kg/mm^2			
Mises Criteria		Tresca Criteria	
(kg/mm^2)	(kg/mm^2)	(kg/mm^2)	(kg/mm^2)
0	0.31	0	0.265
0.1	0.30	0.1	0.26
0.2	0.28	0.2	0.245
0.3	0.25	0.3	0.22
0.35	0.23	0.35	0.20
0.40	0.20	0.40	0.17
0.45	0.16	0.45	0.14
0.50	0.10	0.50	0.09

Von Mises, Tresca and initial yield curves of the polyethylene sample are shown in figure 43.

4.5.2. First Subsequent Yield Curve

When the initial yield curve was obtained, the sample was subjected to extensive plastic deformation under pure tension up to 0.6 kg/mm^2. By this way it was strain hardened and first subsequent yield curve was found experimentally. The stresses for the points of this curve are tabulated in table 26.

Table 26. The stresses for the points of the first subsequent yield curve.

Points	σ (kg/mm^2)	τ (kg/mm^2)
1	0.60	——
2	——	0.49
3	0.53	0.25
4	0.455	0.395
5	0.295	0.49
6	0.12	0.502

The first subsequent yield curve is shown in figure 44.

After obtaining the first subsequent yield curve the sample was loaded in pure torsion. But because of the large elongations in the plastics under loads, the strain gages were damaged and no other yield curves were obtained.

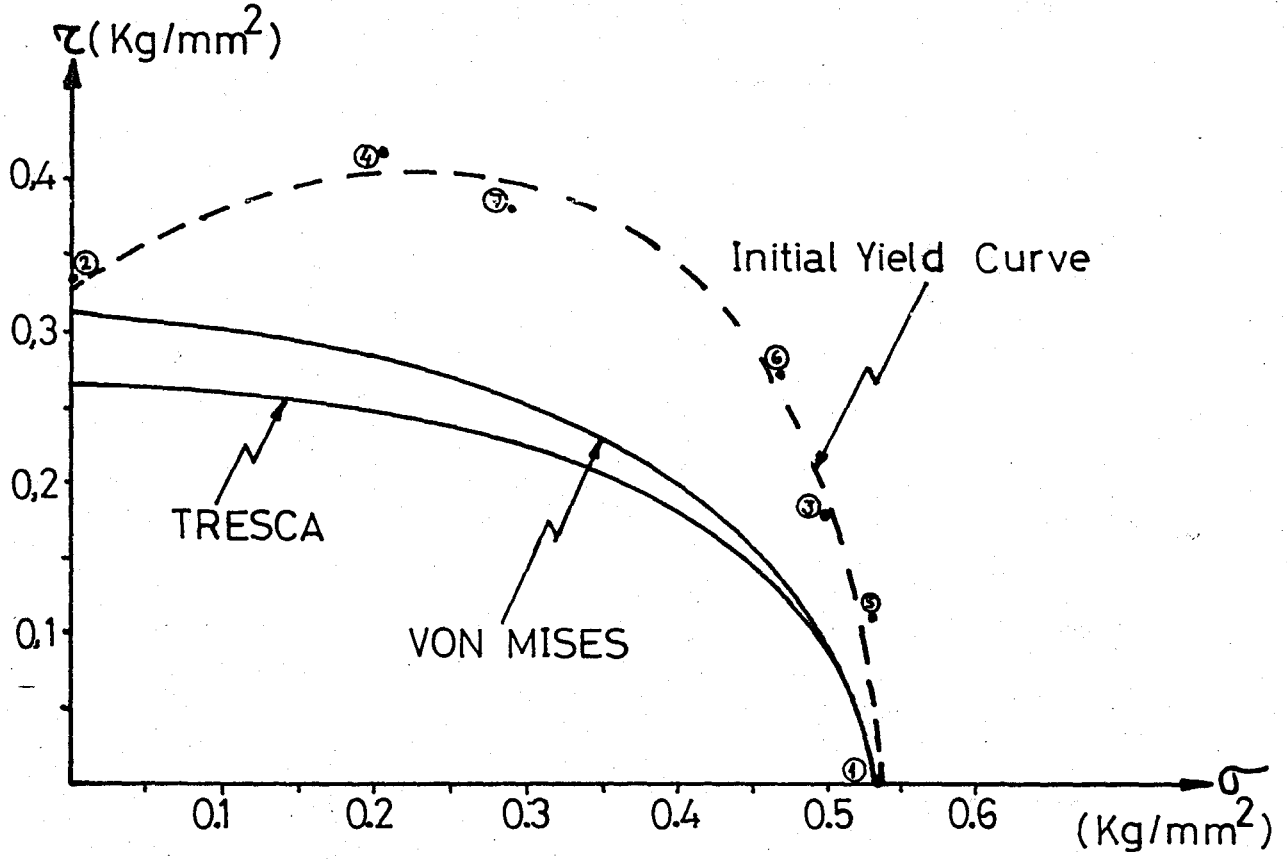

Figure 43. Tresca and von Mises ellipses and initial yield curve of polyethylene.

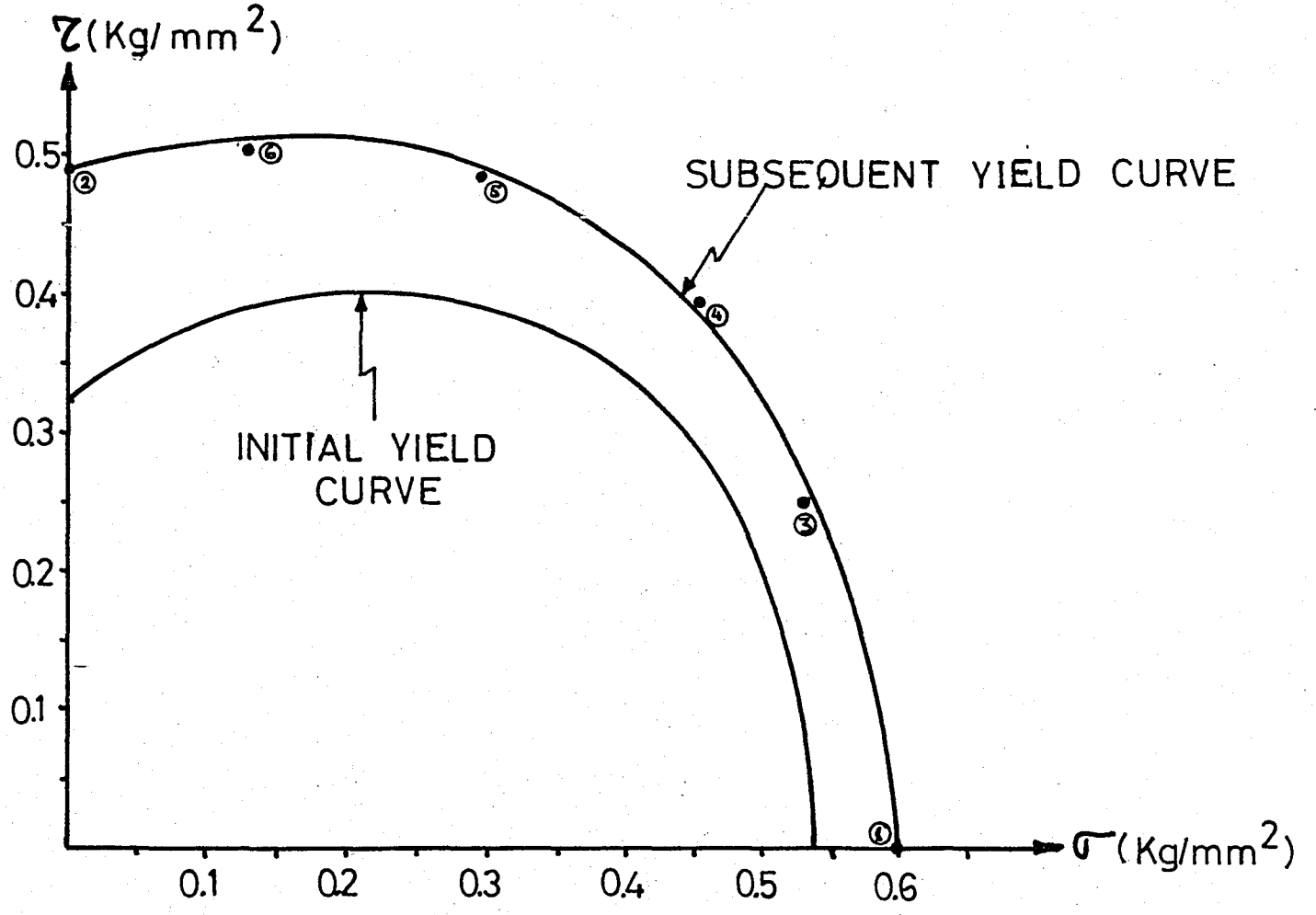

Figure 44. Initial and first subsequent yield curves of polyethylene.

V. DISCUSSION OF EXPERIMENTAL RESULTS

5.1. Annealed Aluminum AA 1100

As it is shown in figure 28, the initial yield curve of annealed aluminum AA 1100 is very close to von Mises ellipse. The similarity between the initial yield curve and Mises ellipse comes from the initial isotropy. There is a small deviation from theoretical curves. The points 7,8,9 of the initial yield curve (Fig.28) are outside the Mises ellipse. The same deviations were found by Taylor and Quinney in 1931, by Lode in 1926, by Ros and Eichinger in 1929 (3), and they concluded that these discrepancies were real and could not be attributed to experimental error or anisotropy of the specimen material.

The subsequent yield curves expanded anisotropically. For the first subsequent yield curve the specimen was strain-hardened under pure tension. The differences between initial yield curve and first subsequent yield curve is small for small tensile stresses and large for large tensile stresses (Fig.29). When it was strain hardened under pure torsion, the yield curve expanded outside for small tensile stresses and the tensile stress of the specimen reduced (Fig.30). So, first and second yield curves intersect each other. For the third subsequent yield curve the sample was plastically deformed once more under pure tension. For this case the yield curve expanded outside for large tensile stresses but for small tensile stresses it reduced as it is

seen in figure 31. When it was strain hardened under proportional loading (shear stress was dominant), the tensile stress reduced but shear stress increased (Fig.32). If the tensile stress would be dominant, the tensile stress of the yield curve probably would be increased.

The normality condition was also observed. For each yield curve, strain vectors were normal to the yield curves. But point five on the initial yield curve, point three on the first subsequent yield curve, points five and 13 on the second subsequent yield curve were not normal. This may be a result of experimental error.

5.2. Cast Aluminum

It is seen from the stress-strain curve of cast aluminum sample (Fig.34) that fracture has occured within the elastic range without any plastic deformation. Since the combined tension-torsion machine requires rather high plastic deformability from materials, cast aluminums can not be tested under combined loadings.

5.3. Extruded ETİAL-60

For extruded ETİAL-60 sample a 60 mm diameter aluminum bar was extruded to 50 mm diameter. After extrusion no heat treatment was performed. So, this sample has an initial anisotropy. The effect of initial anisotropy is seen

in figure 35. Initial yield curve is very different from theoretical yield curves. There is a stress corner around point eight (Fig.35). Subsequent yield curves expanded again anisotropically. At the end of strain hardening under pure torsion the first subsequent yield curve was obtained and seen in figure 36. The tensile stress of initial yield curve increased largely. There is an expansion for small tensile stresses also. For the second subsequent yield curve the sampl was strain hardened under pure torsion. As it is shown in figure 37, the tensile stress reduced. But for small tensile stresses the yield curve expanded outside. First and second subsequent yield curves intersect each other around point three of the second yield curve.

The normality condition was observed for extruded ETİAL-60. Strain vectors are almost normal to the yield curves except a few points.

5.4. Age-Hardened ETİAL-60

The difference between the extruded ETİAL-60 sample and age-hardened ETİAL-60 is only at the heat treatment. For this sample the extruded aluminum bar was age-hardened at 180± 3°C for six hours then air cooled. The effect of age-hardening can be seen by comparing the initial yield curves of extruded and age-hardened ETİAL-60 samples (Fig.35,39). Age hardening increased the yield stresses, especially tensile stress. The tensile stress increased from 4.9 kg/mm^2 to 10.4 kg/mm^2, and shear stress increased from

2.76 kg/mm^2 to 4.48 kg/mm^2. The points 2,5,6,9 and 10 of initial yiled curve (Fig.39) are inside the Tresca ellipse. This may be a result of initial anisotropy. Other points of the initial yield curve are between the Tresca and von Mises ellipses as it is expected. Subsequent yield curves were again expanded anisotropically. The shape of subsequent yield curves depend on the direction of prestraining. For the first subsequent yield curve the sample was strain hardened in the direction of pure tension. So, there is a large increase in pure tension stress (Fig.40). For the second subsequent yield curve, the sample was strain hardened under pure torsion. As a result of strain hardening under pure torsion, there is a drop at the tensile stress and first and second subsequent yield curves intersect eachother. The same result was observed for each sample.

The strain vectors of yield stress points were again normal to yield curves.

5.5. Polyethylene

The initial yield curve of polyethylene (Fig.43) is very different from the theoretical yield curves. Yield stresses of polyethylene are very small compared to the aluminum samples. For example the tensile stress is 0.53 kg/mm^2. The same value was found also by simple tension test. The first subsequent yield curve was found after strain hardening under pure tension (Fig.44). The initial yield curve expanded outside. Because of the large elongations

of polyethylene the strain gages were damaged after obtaining of first subsequent yield curve. For polymer materials any other strain measuring techniques should be used. Because of the difficulties in measuring large strains by strain gages, it was not possible to observe the normality condition.

VI. CONCLUSIONS

1. The effect of initial isotropy on the initial yield curves of the materials was observed. The greater the initial anisotropy, the greater the deviation from theoretical curves.

2. It was observed that Mises criterion yielded better representation for the yield curve of the annealed aluminum which has initial isotropy.

3. The stress corner was observed at the initial yield curve of the extruded ETİAL-60 because of the anisotropy

4. Age hardening increased the initial yield stress significantly. This was observed by comparing the initial yield curves of the extruded ETİAL-60 and age-hardened ETİAL-60 samples.

5. Polyethylene deviated largely from the theoretical curves. Because of the large elongations of the polyethylene, the strain gages were damaged after the obtaining of the first subsequent yield curves. For this kind of study on polymeric materials, other strain measuring techniques should be used.

6. For all materials tested in this study, initial and all subsequent yield curves were found to be convex and smoothand the plastic strain vectors were generally normal

to the yield curves. As a consequence rather few points were sufficient to determine the position of the curve with reasonable accuracy.

REFERENCES

1. M.G. Stout, S.S.Hecker, "An Evaluation of Anisotropic Effective Stress-Strain Criteria for the Biaxial Yield and Flow of 2024 Aluminum Tubes", J. of Engineering Materials and Technology, Vol.105, p.242, 1983.

2. J.Heyman, F.A.Leckie, "Engineering Plasticity", Cambridge University Press, p.206, Cambridge, 1968.

3. J.A.Stricklin, K.J.Sazczalski,"Constitutive Equations in Viscoplasticity", American Society of Mechanical Engineers, Vol.20, pp.1-35, New York, 1976.

4. S.Calayır, "Experimental Study of Plastic Behaviour of Aluminum Under Combined Loading", Master Thesis, Boğaziçi Üniversitesi, 1976.

5. R.A.C.Stater, "Engineering Plasticity", the Gresnam Press, pp.67-88, London,1977.

6. P.W.Bridgman, "Studies in Large Plastic Flow and Fracture", Harvard University Press, p.193, Cambridge, Massachusetts, 1964.

7. W.N.Findley, A.Gjelski, "A Biaxial Testing Machine for Plasticity, Creep or Relaxation Under Variable-Stress Ratios", ASTM Proceedings, Vol.62, pp.1103-1119, 1962.